THE INTERACTION BETWEEN LAMBDA PHAGE AND ITS BACTERIAL HOST

by

Radu Gheorghe Moldovan

BS in Physics, University of Bucharest, 1997

Submitted to the Graduate Faculty of

Arts and Sciences in partial fulfillment

of the requirements for the degree of

PhD in Physics and Astronomy

University of Pittsburgh

2005

UNIVERSITY OF PITTSBURGH

FACULTY OF ARTS AND SCIENCES

This dissertation was presented

By

Radu Gheorghe Moldovan

It was defended on

November 22, 2005

and approved by

Xiao-lun Wu, PhD Professor, Department of Physics and Astronomy

Robert Coalson, PhD Professor, Department of Physics and Astronomy

Robert Duda, PhD Research Assistant Professor, Department of Biological Sciences

Roger Hendrix , PhD Professor, Department of Biological Sciences

David Jasnow, PhD Professor, Department of Physics and Astronomy

Dissertation Director: Xiao-lun Wu, PhD Professor, Department of Physics and Astronomy

THE INTERACTION BETWEEN LAMBDA PHAGE AND ITS BACTERIAL HOST

Radu Gheorghe Moldovan, PhD

University of Pittsburgh, 2005

Our interest in the adsorption of lambda phages onto bacterial cells was triggered by the controversial results Schwartz obtained in the 70's (Schwartz 1976). Lambda phages bind to specific receptors, named LamB, on the cell's surface during the infection process. Phage adsorption onto the cell wall is a diffusion-limited process. One of the controversies is the rate of adsorption, which in some cases appears to exceed the theoretical limit imposed by the physical law of random diffusion. We revisited this problem by carrying out experiments along with new theoretical analyses. Our measurements show that the population of unbound phages decreases with time in a double-exponential fashion. Using fluorescence microscopy we quantified the number of receptors per cell.

This dissertation describes the adsorption of lambda phages onto their host cells and a kinetics model, which allows the calculation of adsorption, desorption, and irreversible binding rates from a single measurement. The long-term interaction between lambda phage and its bacterial host in a co-habitual environment is approached as well. A complex mathematical model describing the dynamics of the two populations (bacteria and phages) is presented along with experimental results. Surprising phenomena of bacterial persistence against phage infection are also reported.

TABLE OF CONTENTS

LIST OF TABLES

LIST OF FIGURES

ACKNOWLEDGMENTS

First I would like to extend my thanks to my research advisor Prof. Xiao-Lun Wu for his patience and guidance through my work, who unconditionally shared his knowledge and support, providing me with lots of insights and best research ideas. I would also like to thank the other members of my committee, Prof. Robert Coalson, Prof. Robert Duda, Prof. Roger Hendrix and Prof. David Jasnow, for their guidance and advice. In particular, I thank Prof. Robert Duda for helping me with technical assistance and discussions for specific biological work. I thank Prof. Chuck Young from Penn State Erie for helping me with theoretical aspects of my work. Also, my thanks are extended to Prof. Roger Hendrix and Prof. Graham Hatfull, for allowing me to use their labs. There, I found very helpful lab personnel. I would like to thank Mr. Brian Firek, Dr. Pallavi Ghosh, Dr. Mariana Piuri, and Dr. Anil Ojha. They provided me with technical assistance and support. I would like to thank all my lab peers for working together and sharing ideas, especially to Dr. Mathew Shtrahman, Emily Chapman, Li Bin and Suddhashil Chattopadhyay.

Finally, I would like to thank to my family, my parents, especially to my wife Roxana, who showed great understanding and encouragement throughout my studies. I dedicate this work to my daughter Victoria.

1.0 INTRODUCTION

The interaction between bacteria and phages has been studied in some detail for many years. Although this topic is a classic one and a lot of knowledge has been accumulated, it is far from being a closed chapter for biologists. At the beginning of the last century, the first bacteriophages were identified independently by F. Twort in 1915 (Twort 1915) and by F. d'Herelle in 1917 (d'Herelle 1917). In 1940, the replicative cycle of bacteriophages was described by Delbruck (Delbruck 1940), and in 1952 it was confirmed by the Hershey and Chase experiment that certain viruses infect bacteria by injecting their DNA into bacteria, leaving their coat behind (Hershey and Chase 1952). This crucial experiment showed that it is the DNA, not the amino acids, that are responsible for heredity. During the last century bacteriophages have played an essential role in our understanding of life phenomena in forms of molecular events, such as DNA structure and the central dogma of molecular biology (Crick and Watson 1970).

1.1 *E. COLI* BACTERIA AND ITS LAMB RECEPTORS

Escherichia coli is a prokaryote, which is a cellular organism that does not have a distinct nucleus. One of the most used in the lab is the gram-negative bacteria *E. coli* K-12. As one can see in figure 1-1, they are enveloped by two membrane systems: inner (plasma) membrane (PM) and outer membrane (OM) separated by periplasmic space. The outer membrane (OM), together

with the peptidoglycan (PG) layer and the periplasm, constitute the gram-negative envelope. The inner or cytoplasmic membrane encloses the cytoplasm, which is the locus for the major metabolic functions including biosynthetic activities. The outer membrane contains two kinds of lipids, lipopolysaccharides (LPS) and phospholipids, as well as some unique proteins (e.g. receptors for bacteriophages) (Beveridge 1999). It contributes to the maintenance of cell shape; and it controls access of nutrient solutes and agents such as antibiotics and detergents to the inner membrane.

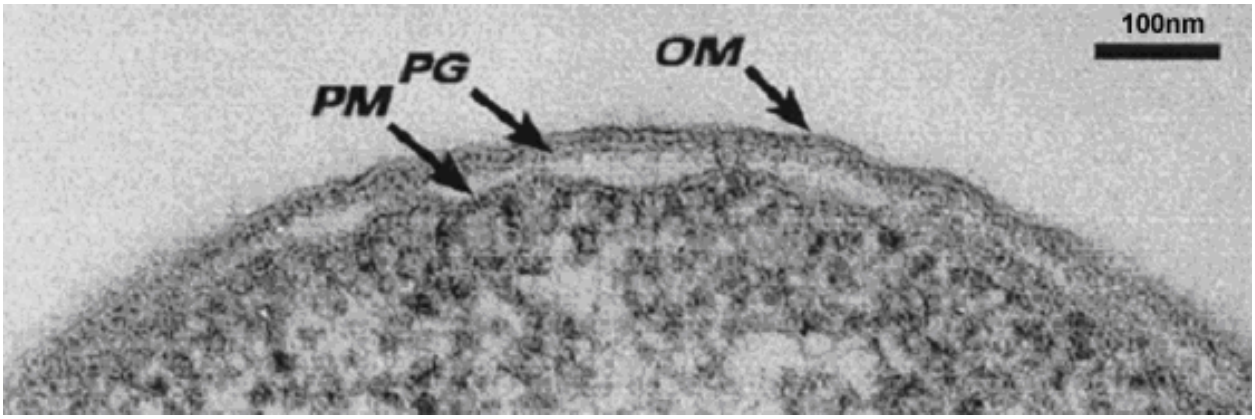

Figure 1-1 Electron micrograph of *E .coli* K-12, adapted from (Beveridge 1999). The periplasmic space is relatively empty of substance, and the peptidoglycan layer (PG), outer membrane (OM), and plasma membrane (PM) can be seen.

E. coli bacteria have many different kinds of receptors on their surface membrane, among which LamB is one. A different name for LamB is maltoporin because it facilitates the diffusion of maltose (360Da) and maltodextrins across the outer membrane (Ferenci and Boos 1980). LamB is an integral outer membrane protein that serves as a cell surface receptor for a number of bacteriophages, including lambda phage (Roa 1979; Charbit and Hofnung 1985). The receptor LamB is a trimer (Nakae and Ishii 1982; Neuhaus 1982), with a molecular weight of 135.6 kDa, looking like a half-open tulip, formed by 3 identical subunits, each one having a molecular weight of 45.9 kDa (Ishii, Okajima et al. 1981). It forms nonspecific channels through the outer

membrane that allow the diffusion of molecules of molecular weights of less than 600Da into the cell. Sequencing of the lamB gene showed that it codes for a 442 amino acid protein with an N-terminal signal sequence, which is cleaved during the biogenesis of the mature protein, resulting in a 421 amino acid polypeptide (Clement and Hofnung 1981). Each subunit monomer in the trimer is an 18 antiparallel β-strand barrel as seen in figure 1-2. The domains highlighted in green, as seen in the stereo picture, figure 1-4, are the sites of mutations that confer resistance to lambda phages (Schwartz 1976; Schirmer, Keller et al. 1995).

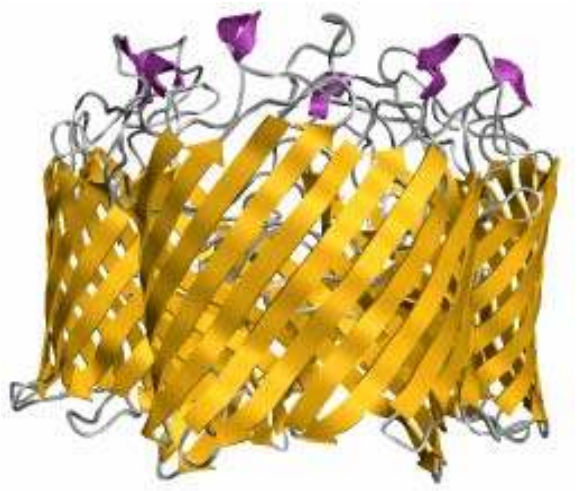

Figure 1-2 Side view of the 18 antiparallel β-strands barrel trimer LamB, adapted from (Schirmer, Keller et al. 1995)

Figure 1-3 X-ray crystallography image of LamB trimer, adapted from RCSB Protein Data Bank http://pdbbeta.rcsb.org/pdb

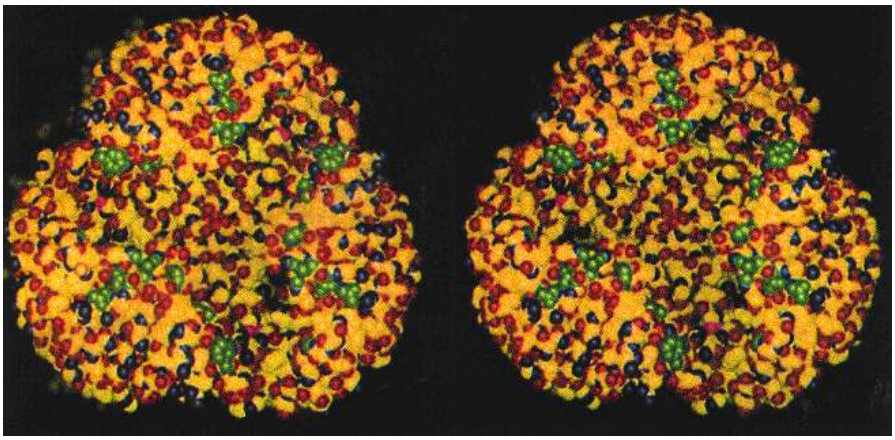

Figure 1-4 Stereo top view of the LamB trimer, adapted from (Schirmer, Keller et al. 1995)

1.2 LAMBDA PHAGE

Like other bacteriophages, lambda phages cannot reproduce themselves autonomously but need the help of a host bacterium to multiply because phages lack the energy metabolism and the

ability to synthesize proteins. Bacteriophage lambda, as seen schematically in figure 1-5, consists of an icosahedrally symmetric (5,3,2 rotational symmetries) head of diameter 60 nm encapsulating the 48,502 bp double strand DNA molecule (Sanger, Coulson et al. 1982) and a somewhat flexible tail through which the DNA passes during infection. Figure 1-6 is an electron micrograph of lambda phages. The tail consists of a hollow tube 135 nm in length, ending in a conical part 15 nm in length, and a tail fiber 23 nm in length, which is attached to the conical part at the distal end of the tail (for a review of lambda tail structure and assembly, see (Katsura 1983)). The tail fiber is composed of two to four copies of polypeptide gpJ. Genetic evidence indicates that gpJ directly interacts with the outer membrane protein LamB during the attachment of the bacteriophage to the surface of the cell. For a review of bacteriophage adsorption see (Schwartz 1980). Some LamB missense mutations (affecting the green domains in the figure 1-4) result in resistance to wild type lambda phage (Thirion and Hofnung 1972). Furthermore, substituting the J gene from lambda with the tail fiber gene from closely related bacteriophage 434 results in a hybrid phage that binds to a different membrane receptor OmpC (Schwartz 1980), the one which phage 434 uses for infection (Fuerst and Bingham 1978). These studies strongly suggest that gpJ determines the host specificity of the phage. More precisely, for the lambda phage case, it is the last 249 amino acids of the gpJ protein sequence which is responsible for the host specificity (Wang, Hofnung et al. 2000). The hollow tube of the tail consists of 32-stacked disks, each of which is formed by six subunits of the major tail protein gpV, arranged such that each disk has a central, 3nm hole. These form the tail channel through which the DNA is expelled during the infection process.

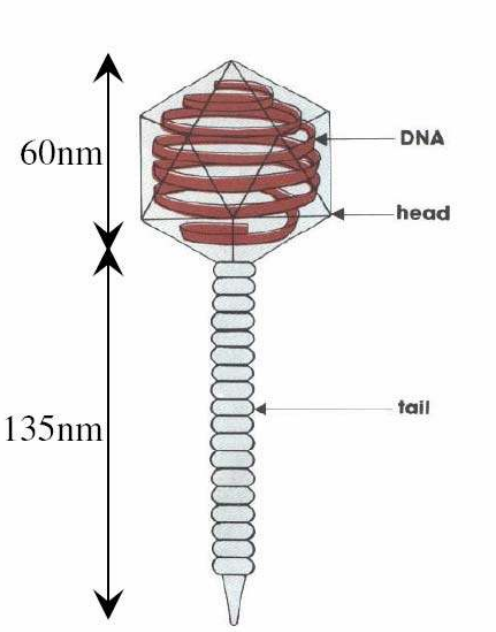

Figure 1-5 Lambda phage cartoon adapted from Genetic Switch, Mark Ptashne

The head and tail are formed independently and join at the last step of assembly, becoming a whole infectious phage. There are mutants that have defective tail genes, producing only phage heads, and also there are mutants that have defective head genes, producing only phage tails. Free phage tails can bind to free heads, yielding viable phages (Weigle 1966). Furthermore, free phage tails binds irreversibly to host cells. Then free heads can attach to the bound tails and inject their DNA normally (Weigle 1968).

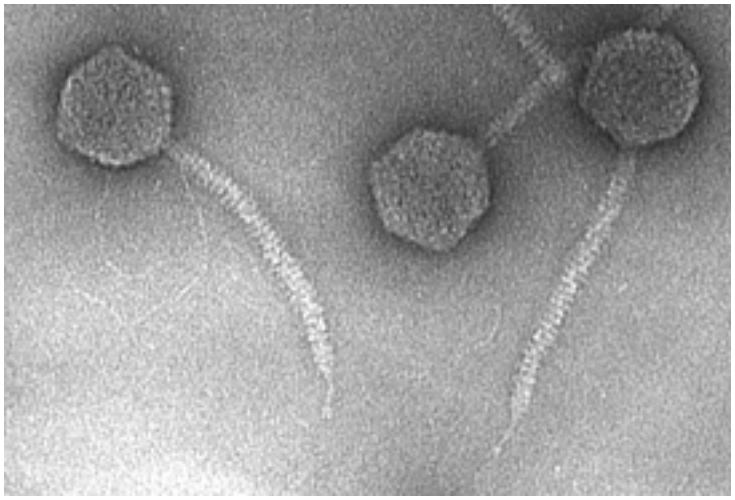

Figure 1-6 Electron micrograph of lambda phages (magnification x100,000) provided by Prof. Hendrix to Genetic Switch, Mark Ptashne

1.3 ADSORPTION AND INFECTION OF LAMBDA PHAGE ONTO *E. COLI*

Lambda phage recruits the maltose (bacterial food) receptor LamB to use for infection. It attaches to this receptor by its tail fiber. The infection process is made of three distinct steps. The adsorption of lambda phages onto bacterial surface is the first step in the infection process (Schwartz 1976). At this initial stage, phages can either dissociate from the host cell in a step called desorption or alternatively bind irreversibly to the host cell (Schwartz 1975). Once the irreversible binding step is triggered, the phage DNA enters the bacterial cytoplasm through the channel formed by the tail, leaving the phage protein capsid behind. The Hershey and Chase Experiment was the first proof that the phage nucleic acid enters the host cell and the phage protein capsid remains outside the host cell. This experiment is famous because it provided strong biological support that DNA is the genetic material (Hershey and Chase 1952). It was proven that the translocation of the DNA could be delayed by lowering the temperature (Mackay

and Bode 1976) or it could be inhibited by $^{+}H_3N\text{-}(CH_2)_4\text{-}NH_3^{+}$ putrescine (Harrison and Bode 1975). Even if the amount of putrescine is not enough to raise the osmotic pressure outside the phage capsid at such extent to prevent ejection, it may inhibit the DNA exit by substituting for the Mg^{2+} in the capsid and forming weak bridges between phosphate groups, thus stabilizing the tertiary structure of condensed DNA and thereby preventing ejection. Extra evidence indicating that the potential energy stored during DNA packaging is used in DNA ejection during the infection process is the fact that varying the external osmotic pressure can inhibit the DNA exit (Evilevitch, Lavelle et al. 2003). However there is also evidence that suggest another protein, such as Pel, may be involved in lambda DNA injection process (Scandella and Werner 1974; Elliott and Arber 1978; Williams, Fox et al. 1986).

Once the lambda phage DNA reaches inside the cell there are two options: lytic growth or lysogenic cycle. Many viruses and bacteriophages follow the lytic pathway, not having the alternative of lysogenic pathways as lambda phage does. Having a lysogenic option makes lambda a temperate bacteriophage. The decision whether to grow lytically or to lysogenize a newly infected bacterium is taken according to the state of the host. It is toward the benefit of the phage to propagate silently, as a part of the lysogen, if the condition for vigorous lytic growth is not optimal (Ptashne 1986).

In the lytic cycle, using the protein synthesis machinery in the host cell, most of the genes on the lambda phage DNA are expressed; this including synthesis of new lambda phage heads, and tails, and replication of many copies of DNA in a concatemer form. At last, the DNA molecules are cut from the concatemer by an enzyme named lambda DNA terminase (Mousset and Thomas 1969), and encapsulated into the heads (Murialdo 1991). Then the tails are attached, and new phages are created. The host cell will die and burst and the new phage crop is released.

This process is called lysis. The new lambda phages can infect other bacteria and a second cycle begins.

In some conditions, for instance in a starving cell, the lysogenic pathway is chosen and the lambda phage chromosome is integrated in the host genome and replicated along with the host genome. The integrated lambda phage is called a prophage. The prophage elaborates a "repressor" protein which prevents expression of most other prophage genes, including those required for lytic growth, by binding to specific control sequence in the prophage DNA. The lambda phage in the lysogenic state can be induced to grow lytically by environmental conditions, such as ultraviolet light or other kind of stress on the cell. Under some stress conditions the so-called SOS response of the cell is triggered. It is known that ultraviolet light damages the DNA molecule, causing RecA, a protein involved in repairing the DNA molecule, to activate an autoproteolytic activity of the lambda repressor, which is responsible for maintaining the lysogenic state. Then the prophage DNA is excised from the cell genome, and starts its lytic cycle. This process is known as induction (Ptashne 1986).

1.4 PHAGE DIFFUSION AND ADSORPTION ONTO CELL SURFACE

Lambda phages have no self-propelling devices to help them move around and reach the LamB receptors on the cell surface. Their motion totally relies on the diffusion or thermal motion, described by Fick's law (see, e.g. **(Berg 1993))**:

$$\vec{J} = -D\vec{\nabla}N_P \qquad (1.1)$$

$$\frac{\partial N_P}{\partial t} = -\vec{\nabla}\cdot\vec{J} \ . \qquad (1.2)$$

First equation (1.1) states that the net flux of phages is proportional to the spatial change in the phage concentration symbolized here by N_P. The dimension for N_P is ml^{-1}. Second equation (1.2) states that the time rate of change in concentration is proportional to the divergence of the current; it is the mass conservation law. In equation (1.1) the proportionality constant D is the diffusion coefficient for phages, which obeys Stokes-Einstein relation:

$$D = \frac{k_B T}{6\pi\eta R} \ , \qquad (1.3)$$

where R is approximately the radius of the phage head, η is the viscosity of the medium, and T is the absolute temperature. Let us assume for now that the cells are ideal spherical adsorbers; therefore there is spherical symmetry, and the Fick's law can be written as:

$$J_r = -D \cdot \frac{\partial N_P}{\partial r} \qquad (1.4)$$

$$\frac{\partial N_P}{\partial t} = D \frac{1}{r^2} \frac{\partial}{\partial r}\left(r^2 \frac{\partial N_P}{\partial r} \right) . \qquad (1.5)$$

In the steady state, the concentration of phages does not change with time, and the boundary conditions are given by: $N_P(a) = 0$ and $N_P(\infty) = N_{P0}$, where a is the cell radius and N_{P0} is concentration of phages far away from the absorbing cell. Notice that we consider the cell to be a perfect adsorber. In other words, all the phages reaching the cell surface are adsorbed, therefore $N_P(a) = 0$. The solution of equation (1.5) and the phage flux from equation (1.4) are given by:

$$J_r(r) = -DN_{P0} \frac{a}{r^2} \qquad (1.6)$$

$$N_P(r) = N_{P0}\left(1 - \frac{a}{r} \right) . \qquad (1.7)$$

The total phage current toward the spherical cell is the inward flux times the cell surface area:

$$I = -J_r(r) \cdot 4\pi a^2 = 4\pi aDN_{P0} \ , \qquad (1.8)$$

and the adsorption rate constant of phages onto cell surface is:

$$k = 4\pi aD \ , \qquad (1.9)$$

which is defined as the probability of adsorption of one phage to one bacterium in 1 ml of solution in 1 second (Schlesinger, 1960; Stent, 1963). Here, k is the maximum adsorption rate, corresponding to the case of totally absorbing cells, that is, the surface of the cell is entirely covered by receptors, the whole cell becoming a spherical sink. For ellipsoidal symmetry, that is for ellipsoidal shaped cells, the same kind of calculation will lead to a maximum adsorption rate (Berg 1993):

$$k = 4\pi aD/\ln(2a/b) \ , \qquad (1.10)$$

where $a(>b)$ and b are the semi axes of the ellipsoid. Notice that the factor $1/\ln(2a/b)$ does not make a huge difference compared to the spherical cell case. For example, for a 4μm long and 1μm thick bacteria the factor $1/\ln(2a/b)$ is 0.48. Therefore, from the adsorption point of view, considering cells to be spherical will not change k by orders of magnitude. Actually for a number of receptors per cell that is not very large, it can be shown that cell shape does not affect the adsorption rate at all, as seen in equation (2.41), only the maximum adsorption rate, which is the case for the cell all covered with receptors, would be affected. However, let us consider for now that the theoretical upper limit of the adsorption rate, purely based on random three-dimension diffusion is:

$$k_{\max} = 4\pi aD \ . \qquad (1.11)$$

This theoretical result was first derived by Smoluchowski in 1917 (von Smoluchowski 1917). It is interesting to point out the Schwartz experiment (Schwartz 1976), which indicated that this limit could be exceeded. First to notice this was Berg and Purcell (Berg and Purcell 1977). They introduced a hyperbolic model for the adsorption rate dependence on the number of receptors based on an electrical capacitance analogy (Berg 1993). The correction factor C is introduced to adjust the adsorption rate for the real case when the cell is not a perfect sink, i.e. only a finite number of receptors:

$$k = k_{\max} C$$
$$C \equiv \frac{Ns}{Ns + \pi a} \quad . \qquad (1.12)$$

Here, N is the number of receptors per cell and s is the size (radius) of the LamB receptor. Fitting Schwartz data with this model one can get $k_{max}=2.19\cdot10^{-10}cm^3/s$, as can be seen in figure 1-7. The size of the LamB receptor can also be obtained from the fitting: $s=4.65nm$. This is consistent with modern structural measurements of s≅4nm, obtained by using Web Mol Applet (x-ray crystallography structure) from RCSB Protein Data Bank: http://pdbbeta.rcsb.org/pdb/, as can be seen in figure 1-8. More precisely, considering the cells as elliptical shape, the correction factor C and k_{max} are:

$$k_{\max} = 4\pi a D / \ln(2a/b)$$
$$C \equiv \frac{Ns}{Ns + \pi a / \ln(2a/b)} \quad ,$$

which provides a different value for fitting parameter $s=4.01nm$, based on using $a=8\cdot10^{-5}cm$ and $b=5\cdot10^{-5}cm$ for the semi axes of the ellipsoidal cell.

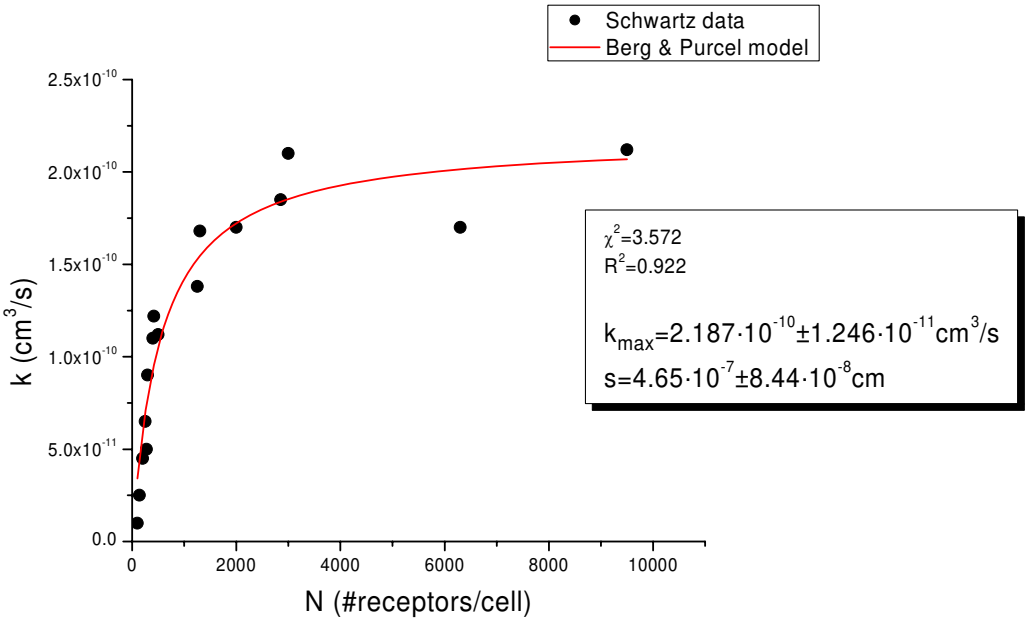

Figure 1-7 Schwartz data fitted by Berg and Purcell model

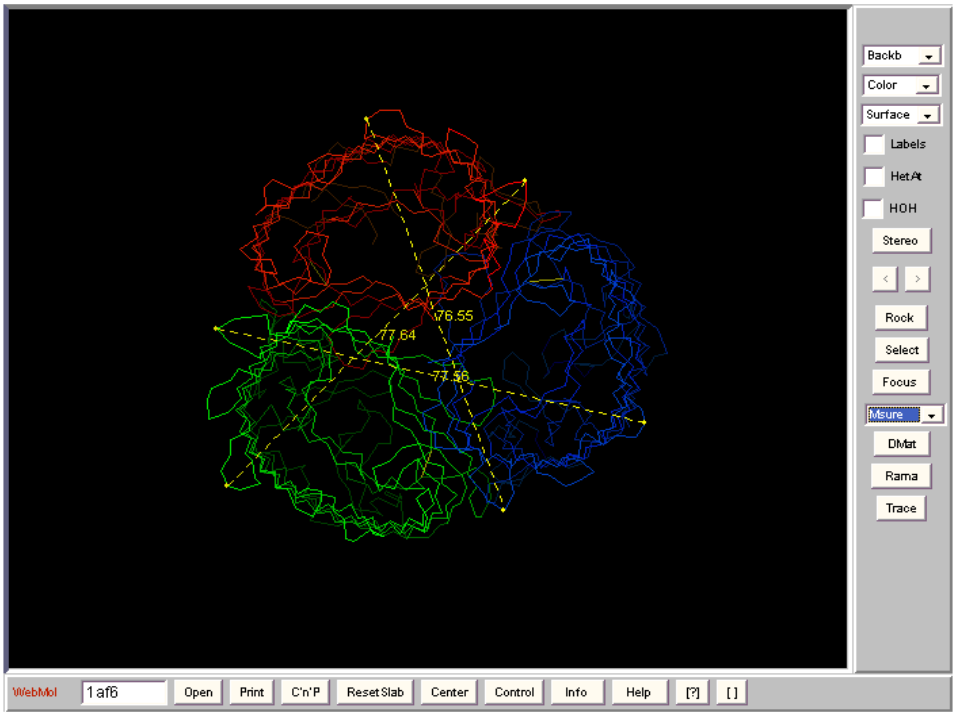

Figure 1-8 LamB X-ray crystallography representation (top view), showing the size of the receptor. For simplicity only the backbone structure is shown. Image obtained by using Web Mol Applet from RCSB Protein Data Bank

Estimation of LamB receptor size by fitting Schwartz data by Berg & Purcell model (see figure 1-7), was obtained by using a cell size of $a=8\cdot10^{-5}$cm , as Schwartz reported. This value seems small compared to the size of the same strain cells grown in our lab. Using a cell size value we observed of $a=2\cdot10^{-4}$cm , LamB receptor size would be $s=11.6$nm , almost three times larger than the known LamB size. But this could be just an "effective" size of the receptor, considering the logic of the model. In other words this would be the "hot" area on the cell surface which being touched by the phage tail will result in irreversible binding.

Actually, the very high adsorption rate Schwartz measured compared to the theoretical limit he calculated using $k_{\max} = 4\pi aD$, might be due to the small cell size value he used in his calculations. For $a=8\cdot10^{-5}$cm , the theoretical upper limit for the adsorption rate given by equation (1.11) is $k_{max}=7.3\cdot10^{-11}\text{cm}^3/\text{s}$ which is exceeded by Schwartz experimental adsorption rate $k_{max}=2.19\cdot10^{-10}\text{cm}^3/\text{s}$ by a factor of 3. Again, a more accurate estimation, using equation (1.10), which describes the maximum adsorption for an elliptical cell, one gets even lower $k_{max}=6.3\cdot10^{-11}\text{cm}^3/\text{s}$. In any event, using a cell size value of $a=2\cdot10^{-4}$cm , matching our cells, the theoretical limit for the adsorption rate is $k_{max}=1.26\cdot10^{-10}\text{cm}^3/\text{s}$ for cells to be spherical or $k_{max}=6.06\cdot10^{-11}\text{cm}^3/\text{s}$ for cells to be ellipses. For even large cell size, $a=4\cdot10^{-4}$cm , for which the theoretical limit is $k_{max}=9.09\cdot10^{-11}\text{cm}^3/\text{s}$ (estimation for the elliptical cells case, equation (1.10)) the experimental value $k_{max}=2.19\cdot10^{-10}\text{cm}^3/\text{s}$ cannot be exceeded by the theoretical prediction. It is difficult to conclude whether the Schwartz cells were very small or of reasonable size. Although a small cell size of $a=8\cdot10^{-5}$cm is hard to believe, especially when we grow the same strain of cells using the same conditions. Either way, the measured adsorption rate is exceeding the calculated maximum adsorption rate.

In the above calculations of maximum adsorption rate we considered the lambda phage as a spherical particle of 60μm diameter, therefore its 3D diffusion coefficient in aqueous solution (η=.01Poise) at room temperature would be:

$$D = \frac{k_B T}{6\pi\eta R} = 7.3 \cdot 10^{-8} cm^2 / s \ . \qquad (1.13)$$

We have to mention that this estimated result for considering lambda phage as a sphere, no tail, is in good agreement with the light scattering measurement, yielding $D = 6.8 \cdot 10^{-8} cm^2 / s$ (Wu, personal communication).

Suppose that Schwartz cells were of radius a=$8 \cdot 10^{-5}$cm and therefore the maximum adsorption rate k_{max}=$7.3 \cdot 10^{-11}$cm^3/s , the discrepancy between this value and the experimental value may be explained if Schwartz's bacteria were swimming cells, with a velocity of 128μm/s. This value was obtained by extrapolating the plot of phage absorption as a function of bacterial swimming velocity. This plot, as seen in figure 1-9, is adapted from (Berg and Purcell 1977). It is plotted as $J / J_0 - 1$, the fractional increase in the current collected by a moving sphere compared to that collected by a stationary sphere, against av / D, the dimensionless velocity. Here, a is the cell radius and D is the diffusion coefficient of the absorbed molecules, lambda phages in our case. The current J of adsorbed molecules to the cell is defined as $J = k_{\max} c_\infty$, where c_∞ is the concentration of molecules faraway from the adsorber. Therefore one can write:

$$\frac{J}{J_0} - 1 = \frac{k_{\max}}{k_{\max 0}} - 1 = f\left(av / D\right) , \qquad (1.14)$$

where f is a function describing the relationship between the current of adsorbed molecules and the velocity of the spherical adsorber. In order to have an increase of factor 3 in the adsorption rate, which is needed to explain the high experimental value Schwartz obtained, the value of the

function f has to be 2 as seen from equation (1.14). Therefore the argument av/D can be obtained from linearly extrapolating the plot of $f(av/D)$, as can be seen in figure 1-9 (i.e. the red value),

$$\frac{k_{\max}}{k_{\max 0}} = 3 \Rightarrow av/D = 14 \Rightarrow v = 128\mu m/s \ . \qquad (1.15)$$

This is a huge velocity for a bacterium to reach. The strain *E. coli* RP437, considered to be a good swimmer, possesses an average velocity of 20μm/s (Wu and Libchaber 2000). Therefore it is impossible for the bacteria utilized by Schwartz to show such an outstanding swimming ability.

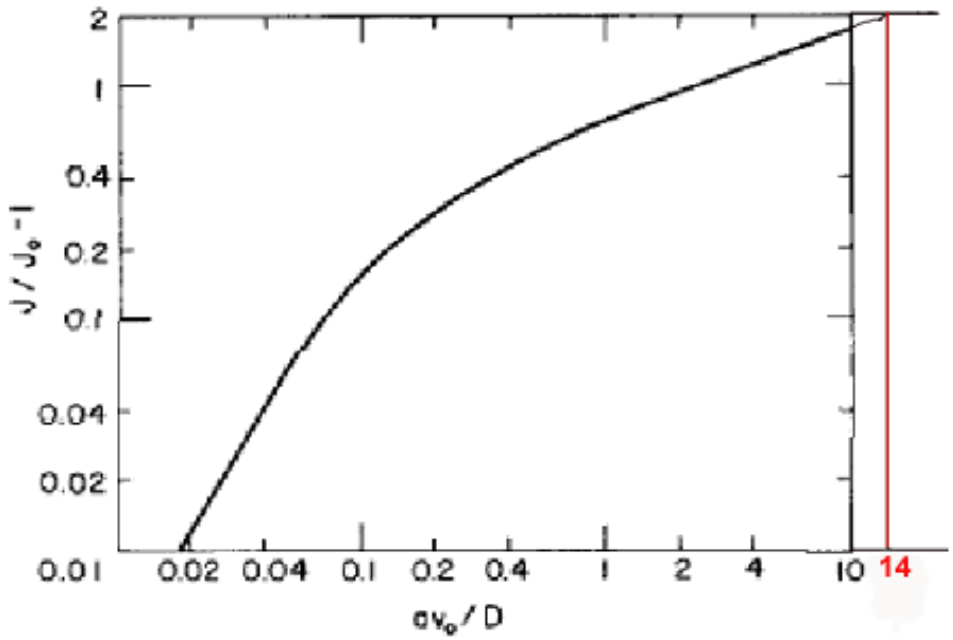

Figure 1-9 Figure adapted from (Berg and Purcell 1977) showing the fractional increase in current $J/J_0 - 1$ to a spherical adsorber of radius a, as av_0/D dependence. J and J_0 are the currents collected by moving (at velocity v_0) and stationary spherical absorbers, respectively. D is the diffusion coefficient of the molecules adsorbed.

A striking feature of phage adsorption confirmed by both Berg & Purcell hyperbolic model and Schwartz data is the fact that for relative small number of well dispersed receptors, corresponding to a small fraction of the cell surface, the adsorption approaches the theoretical limit. Remember that the maximum adsorption rate is obtained for the case of the cell being completely covered by receptors, meaning the cell is an ideal sink for the phages. For example an adsorption rate of half of its theoretical limit can be achieved by $N=\pi a/s$ from equation (1.12). For Schwartz cells of size $a=8\cdot10^{-5}$cm and $s=4nm=4\cdot10^{-7}$cm, the number of receptors per cell for which half of the maximum adsorption is reached will be $N=630$, which is in close agreement with Schwartz data, as can be seen in figure 1-7. $N=630$ receptors corresponds to only $(N\pi s^2/\pi a^2)\cdot100\%=1.6\%$ of the total cell surface. This means that many different types of receptors can be accommodated on the cell surface and all are very efficient. For our cells $a=2\cdot10^{-4}$cm, the number of receptors per cell for which half of maximum adsorption is reached will be $N=1600$. It is important for the receptors to be well dispersed. If they were aggregated into a single big circular patch of the same total area instead of being uniformly dispersed (as in a lattice), the adsorption rate of half of its theoretical limit would be reduced from $k_{max}/2$ to $k_{max}/(630)^{1/2}=k_{max}/25$ due to area issue. If the receptors were randomly dispersed the adsorption rate will not be much different, less than a few percents compared to the uniformly dispersed case, as long as the number of receptors per cell is higher than 50 (Berg and Purcell 1977). Here, by randomly dispersed it is meant that the distance between receptors on the cell surface is a random variable. And by uniformly dispersed it is meant that the distance between receptors don't vary at all, being arranged in a uniform lattice. In both cases the average distances between receptors are comparable.

1.4.1 Two-stage capture

It has been speculated that bacterium and phages coevolved such that the binding is highly optimized. This speculation is motivated by the observation of very high adsorption rate approaching the theoretical limit predicted by random spatial diffusion. It was suggested by Delbruck that one of the possible optimizations is a two-stage capture process (Adam and Delbruck 1968). In order to efficiently bind to a receptor, which is very small compared to the size of a bacterium, the phage particle first finds the bacterium by 3D diffusion, and then on the cell surface, it diffuses two-dimensionally until it reaches a receptor. During the surface diffusion the bacteriophage has the chance to desorb before being captured.

The advantage of this two-stage process was questioned and analyzed by Berg and Purcell (Berg and Purcell 1977). By comparing the diffusion currents for pure 3D diffusion vs. 3D+2D diffusion they concluded that in order for the two-stage capture model to be advantageous, the binding energy between bacterium and phage has to be strong enough that the phage remains on the surface but weak enough so that it can diffuse two-dimensionally.

The theoretical prediction of Adam and Delbruck (Adam and Delbruck 1968), such as dimensional reduction can enhance the reaction rates is not always true. As can be seen in Figure 1-10, it depends on two facts. One is the ratio of the 2D to 3D translational diffusion coefficients D_2/D_3; the other one is the ratio of diffusion space size to target size b/a. The contours plotted in Figure 1-10 represents three different values (0.1, 1.0 and 10) for the ratio of the mean lifetimes of the reactants t_{2+3}/t_3 for theoretical two-step (3D+2D) vs. one-step (3D) searching process. Obviously, $t_{2+3}/t_3<1$ corresponds to an advantageous two-stage process, whereas $t_{2+3}/t_3>1$ corresponds to an impeding one (i.e. the stippled region in Figure 1-10). The 2D diffusion should not be very different from bulk diffusion in the case of the lambda phage considering the fact

only the tail tip is bound to the membrane while the head, the bulkiest part of the phage, is diffusing outside of the membrane (giving about the same viscosity for both 2D and 3D cases). Therefore a D_2/D_3 value in the range of [0.1-1] is appropriate. The diffusion space size b is the distance between neighboring receptors on the cell surface. As it will be shown in the next two chapters, our cells have ~130 receptors per cell, and are ~4μm in length and ~0.8μm in diameter. Therefore, b can be estimated as ~250nm, whereas the target (LamB receptor) radius is 4nm based on x-ray crystallography measurements (as seen in Figure 1-8) and thus the ratio b/a is ~60. Based on these estimations the adsorption rate of lambda phages onto our cells (i.e. ~130 receptors per cell) should be enhanced by reduction of dimensionality. In other words the adsorption of lambda phages should be a 3D diffusion limited process.

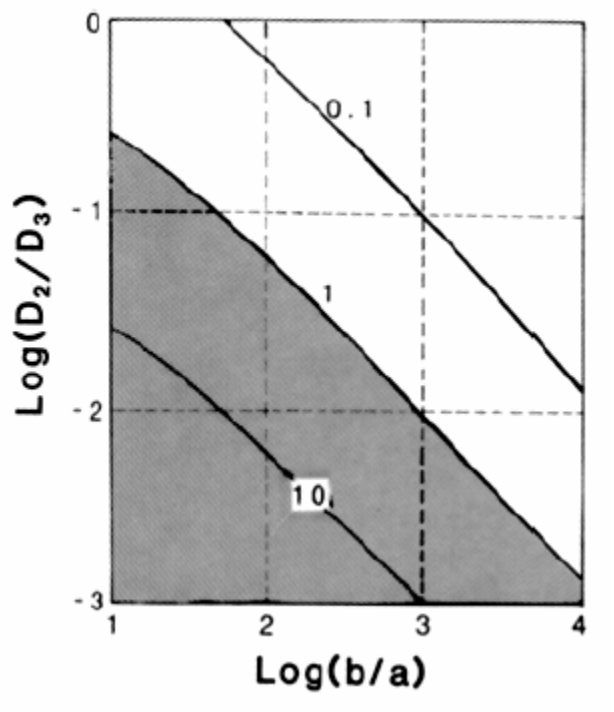

Figure 1-10 Reduction of dimensionality can enhance or impede the reaction rates depending on the ratio of 2D to 3D diffusion coefficients D_2/D_3 and the ratio of diffusion space size to target size b/a; figure adapted from (Adam and Delbruck 1968)

In contrast, we experimentally observed that the phage adsorption is actually not enhanced by the reduction of dimensionality, but rather slowed down due to a slow irreversible binding rate to the receptor. Therefore the limiting step in lambda phage infection process is not the bulk diffusion as theoretically predicted by the two-stage capture model of Adam and Delbruck (Adam and Delbruck 1968), but rather the low binding probability to the receptor. This kind of process is called a reaction limited process (Axelrod and Wang 1994), based on the inability of the receptor to bind to the ligand after every collision. Adam and Delbruck (Adam and Delbruck 1968) theory takes into account a perfect adsorber, which means all Brownian collisions leads to binding. This usually is not the case in real life. For the case of LamB receptor, based on our adsorption measurements (see next chapter), we believe that its irreversible binding ability is far from being perfect; only a small fraction of the collisions lead to irreversible binding. The time scale of desorption and/or irreversible binding of phages in our adsorption experiments (i.e. $\sim 10^3$s) is much longer than the diffusion time (i.e. ~1s) needed by the phage during the 2D search to find its receptor and thus we assume that the chance of phage desorption from the cell while 2D searching is very small. Most of the desorptions happen after the encounter with the receptor. Our experimental results standing against the theoretical two-stage capture model prediction (which uses a perfect adsorber description) are supported by other reports (McCloskey and Poo 1986). Therefore the probability of successful irreversible binding per collisional encounter is a key parameter in determining the efficiency of reduction dimensionality enhancement.

2.0 ADSORPTION EXPERIMENT

Knowing how fast viruses are able to successfully infect bacteria is an important issue. Similarly important is the infection mechanism. This knowledge will aid in the design of defense strategy against viral infection. Therefore understanding the kinetics of virus adsorption to the cell is important.

2.1 EXPERIMENTAL PROCEDURE

We designed an experiment that allows us to measure the number of free phages as a function of incubation time. We set up 12 adsorption reactions containing lambda phages and bacteria for 12 different incubation times. All the reactions are stopped simultaneously by a ~50 fold dilution. Then diluted incubation samples are quickly spun at highest speed (~16000rcf) for one minute. This spinning is not meant to form a sturdy pellet, but to clear the top part of the diluted sample from most of the infected cells; therefore only free phages are carefully sampled out at this point. It is not possible to sample from all 12 samples at once without introducing fluctuations in the number of free phages due to resuspension of pellet containing infected cells. Therefore sampling out from 4 centrifuge tubes at once, seems to be on the safe side. Then again a very fast spin for one minute will allow sampling out of free phages from the next 4 centrifuge tubes, and so on so forth. It is very important to be fast in performing this experimental procedure because

time is an experimental variable. The length in time of our adsorption experiment is shorter than the latent time, which is the time needed by an infected cell to produce and release by lysis a new crop of phages. Therefore the total number of phages in the reaction is not altered by new produced phages. Once all 12 different free phages samples are obtained after different incubation times, they are titered using standard methods. First the free phages samples are incubated with control bacteria in adsorption buffer (10mM $MgSO_4$, pH=7.4) for 15 minutes. Then using the agar overlay technique each free phage will produce a clear plaque, such that their concentrations can be quantified.

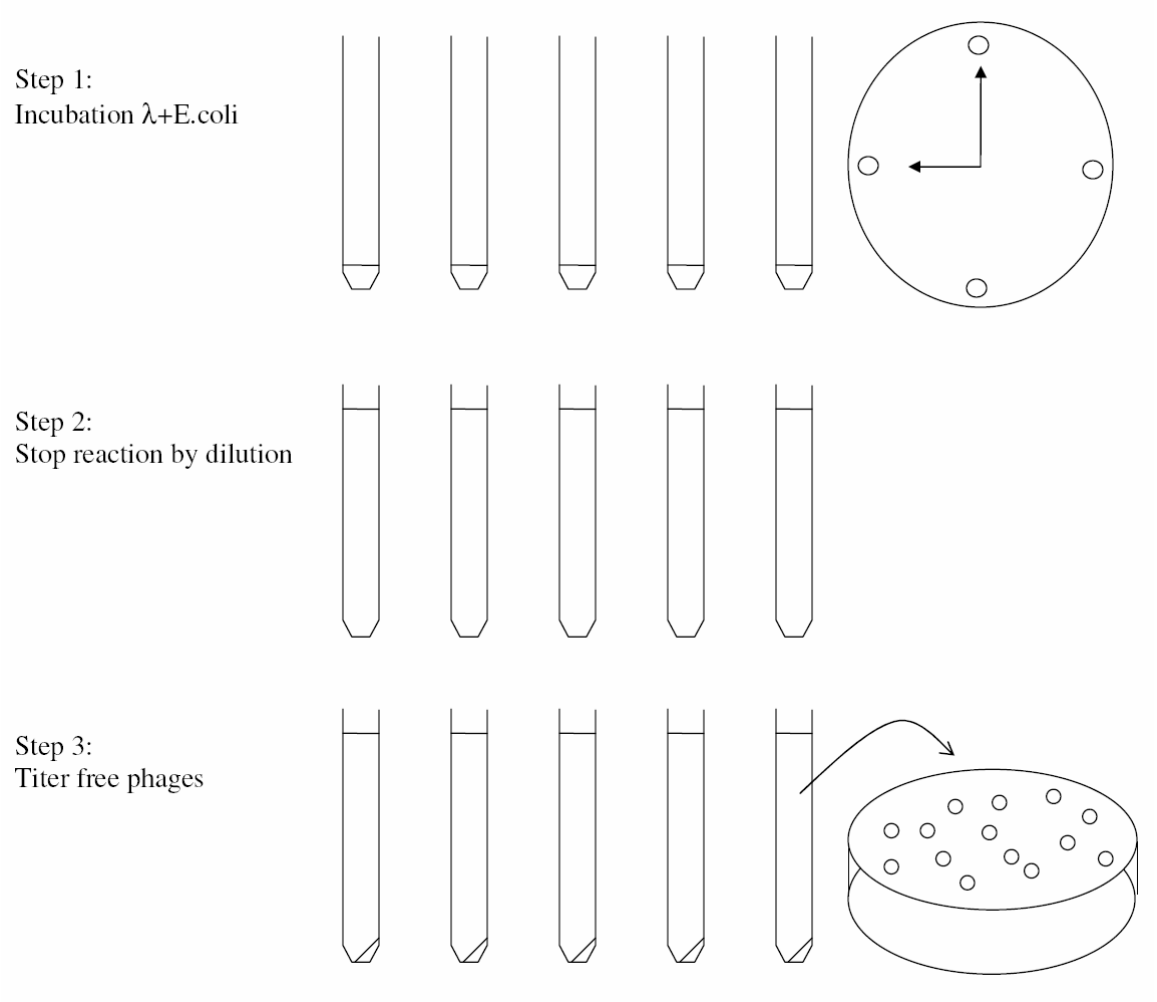

Figure 2-1 The three stage adsorption experiment

In the sketch above showing the three stages of the adsorption experiment, one can see that after incubation of cells and phages for different amounts of time (stage 1), all reactions are stopped by dilution (stage 2), and then spun down in order to allow only free phages to be sampled out and titered (stage 3). The number of tubes corresponds to the number of reactions set up for different times. In the sketch, for simplicity only 5 tubes are drawn. In the actual experiment we used 12 tubes. Another detail worth to be mentioned is about the pellets drawn at the bottom of the tubes in the last stage. They are exaggerated. In reality they are invisible. Otherwise stopping the reaction by dilution would not be efficient. Although an intuitive sketch is presented in figure 2-1, the reader should refer to Materials and Methods in Appendix for a detailed protocol.

2.2 THE ADSORPTION MODEL

Assuming phage adsorption obeys kinetics of first order reaction:

$$B + P \underset{k'}{\overset{k}{\rightleftarrows}} BP \xrightarrow{k''} BP^* \ ,$$

where B and P stand for the two reactants: bacteria and phages, and BP and BP* stand for the the products of the reaction: reversibly bound complexes and irreversibly bound complexes. Let us mention that in our adsorption experiment the irreversibly bound complexes coincide with the infected bacteria. Once the irreversibly binding happen the DNA injection is triggered and they immediately become infected bacteria. One can describe the reaction by the following system of differential equations:

$$\frac{dN_{BP}}{dt} = kN_B N_P - \left(k' + k''\right) N_{BP} \qquad (2.1)$$

$$\frac{dN_P}{dt} = k' N_{BP} - kN_B N_P \qquad (2.2)$$

$$\frac{dN_B}{dt} = k' N_{BP} - kN_B N_P \qquad (2.3)$$

$$\frac{dN^*_{BP}}{dt} = k'' N_{BP} \ , \qquad (2.4)$$

where N_{BP} is the concentration of transient (reversibly bound) bacterium-phage complexes,

N_P is the concentration of free phages,

N_B is the concentration of free bacteria,

N^*_{BP} is the concentration of infected bacteria,

k is the adsorption rate constant,

k' is the desorption rate constant,

k" is the irreversible binding rate constant

This set of ODE (ordinary differential equations) is valid for low MOI (multiplicity of infection = $N_P/N_B << 1$), which means no multiple infections for a single bacterium. The first term on the right hand side of equation (2.1) represents the source of transient bacterium-phage complexes BP created by adsorption of phages onto cells at rate k. Always, the source term is a positive one. The next two negative terms in equation (2.1), are the sink terms. The transient bacterium-phage complexes are decaying by desorption of phages from cells (dissociation) back into a free phage and a free bacterium at rate k', or become an irreversibly bound complex at rate k". In the same fashion all the other equations (2.2), (2.3) and (2.4) can be described. Notice that there is no production terms for phages or bacteria. The adsorption experiment is performed in adsorption buffer (10mM $MgSO_4$, pH=7.4), and not in

growth media, therefore the cell division is negligible. The length in time of adsorption experiment is shorter than the time needed for the infected cells to produce new crop of phages, therefore no phage production term in our adsorption model.

We have to mention that the irreversible binding step is not the same step as the phage DNA translocation step. There is experimental evidence to show that DNA translocation can be stalled by external means, while the phages are irreversibly bound to bacteria (Mackay and Bode 1976). The irreversible binding step is the necessary step before the phage DNA translocation. However, our experiment can not address issues related to late-stage infection. New measurements are needed to study this crucial step.

Let us examine the asymptotic behavior as $t \to \infty$ and $dN/dt \to 0$ for the above ODEs.

For $k'' \neq 0$, equation (2.4) implies $N_{BP}^{\infty} = 0$ and then from all the other equations is inferred that $N_P^{\infty} = 0$ ($N_B^{\infty} = 0$ is ruled out because MOI<<1, that is $N_B >> N_P$). Thus for $k'' \neq 0$, equation (2.4) sets up a sink for phage particles.

For $k''=0$, equation (2.1) implies that the equilibrium of free phages and transient complexes will be reached and the equilibrium constant, defined as the ratio of products' and reactants' concentrations is $K_a = N_{BP}^{\infty} / N_B^{\infty} N_P^{\infty} = k / k'$.

The conservation of the number of the particles holds at all time: $\Delta N_B = \Delta N_P$. So, one can write the concentration of free phages and of uninfected bacteria at time t:

$$N_P(t) = N_P^0 - N_{BP}(t) - N_{BP}^*(t) \qquad (2.5)$$

$$N_B(t) = N_B^0 - N_{BP}(t) - N_{BP}^*(t) \ , \qquad (2.6)$$

where N_P^0, N_B^0 are for t=0.

Substituting equations (2.5) and (2.6) into equation (2.1) one finds:

$$\frac{dN_{BP}}{dt} = k\left[N_{BP}^2 - \left(N_B^0 + N_P^0 + \frac{k'+k''}{k} \right) N_{BP} + N_B^0 N_P^0 + N_{BP}^{*2} - (N_B^0 + N_P^0 - 2N_{BP}) N_{BP}^* \right] . \quad (2.7)$$

As one can see this is a nonlinear differential equation, which usually offers multiple solutions. In order to close the system and linearize equation (2.7) we use the condition MOI<<1 along with equations (2.5) and (2.6); i.e. $N_B >> N_P > N_{BP} > N_{BP}^*$. Therefore, the following terms: N_{BP}^2, N_{BP}^{*2}, $N_{BP} \cdot N_{BP}^*$, $N_P^0 \cdot N_{BP}$ and $N_P^0 \cdot N_{BP}^*$ will be neglected. This linearization procedure is completely consistent with our experimental conditions.

Then equation (2.7) becomes:

$$\frac{dN_{BP}}{dt} = k\left[-\left(N_B^0 + \frac{k'+k''}{k} \right) N_{BP} + N_B^0 N_P^0 - N_B^0 N_{BP}^* \right] . \quad (2.8)$$

Taking the time derivative of both sides, one finds:

$$\frac{d^2 N_{BP}}{dt^2} = k\left[-\left(N_B^0 + \frac{k'+k''}{k} \right) \frac{dN_{BP}}{dt} - N_B^0 \frac{dN_{BP}^*}{dt} \right] . \quad (2.9)$$

One can replace the time derivative in the last term of equation (2.9) by using equation (2.4).

$$\frac{d^2 N_{BP}}{dt^2} + k\left(N_B^0 + \frac{k'+k''}{k} \right) \frac{dN_{BP}}{dt} + kk'' N_B^0 N_{BP} = 0 . \quad (2.10)$$

Equation (2.10) along with the initial conditions: $N_{BP}(0)=0$ and $dN_{BP}(0)/dt = kN_B^0 N_P^0$ uniquely determine the time evolution of the population of transient bacterium-phage complexes during the adsorption process. It is interesting that equation (2.10) has the mathematical form of a damped harmonic oscillator and allows the solution $N_{BP} = a \cdot \exp(i\omega t)$ with first and second derivatives as $\frac{dN_{BP}}{dt} = ai\omega \cdot \exp(i\omega t)$ and $\frac{d^2 N_{BP}}{dt^2} = -a\omega^2 \cdot \exp(i\omega t)$, respectively. Notice that ω is purely imaginary as shown below and thus no need to use the real part notation for the description of transient (reversibly bound) bacterium-phage complexes $N_{BP} = \mathrm{Re}[a \cdot \exp(i\omega t)]$.

Using this exponential solution for equation (2.10), we find:

$$-a\omega^2 \cdot \exp(i\omega t) + k\left(N_B^0 + \frac{k'+k''}{k}\right) ai\omega \cdot \exp(i\omega t) + kk'' N_B^0 a \cdot \exp(i\omega t) = 0 \ , \tag{2.11}$$

and it simplify to:

$$\omega^2 - k\left(N_B^0 + \frac{k'+k''}{k}\right) i\omega - kk'' N_B^0 = 0 \ . \tag{2.12}$$

The solution to the quadratic equation is:

$$\omega_{+/-} = \frac{i}{2}\left[\left(kN_B^0 + k'+k''\right) \pm \sqrt{\left(kN_B^0 + k'+k''\right)^2 - 4kk'' N_B^0}\right] \ . \tag{2.13}$$

It can be shown that the expression under the square root in the equation (2.13) is positive, by rearranging the terms. $\left(kN_B^0 + k'+k''\right)^2 - 4kk'' N_B^0 = \left(kN_B^0 - k''\right)^2 + k'^2 + 2kk' N_B^0 + 2k'k'' \geq 0$, since all three rates and the initial bacteria concentration are positive. Therefore ω is purely imaginary.

It can be shown that the solution for equation (2.10) is of the form

$$N_{BP}(t) = a \cdot \exp\left(-t/\tau_1\right) + b \cdot \exp\left(-t/\tau_2\right) \tag{2.14}$$

with $1/\tau_{1,2} = -i\omega_{+/-}$ or:

$$\begin{aligned} \frac{1}{\tau_1} &= \frac{1}{2}\left[\left(kN_B^0 + k'+k''\right) + \sqrt{\left(kN_B^0 + k'+k''\right)^2 - 4kk'' N_B^0}\right] \\ \frac{1}{\tau_2} &= \frac{1}{2}\left[\left(kN_B^0 + k'+k''\right) - \sqrt{\left(kN_B^0 + k'+k''\right)^2 - 4kk'' N_B^0}\right] \end{aligned} \ . \tag{2.15}$$

One can see that there are two decay times τ_1 and τ_2. The τ_1 is the short relaxation time and τ_2 is the long relaxation time. Both take real values since the expression under the square root in equation (2.15) is positive as shown above. It is obvious that $\left[\left(kN_B^0 + k'+k''\right) \geq \sqrt{\left(kN_B^0 + k'+k''\right)^2 - 4kk'' N_B^0}\right]$, since all three rates and the initial bacteria concentration are positive. This makes the two relaxation times to be positive, which is expected.

Let us mention here the degenerate case of $\tau_1 = \tau_2 = \tau$. This happens when $\sqrt{\left(kN_B^0 + k' + k''\right)^2 - 4kk''N_B^0} = 0$ and using simple algebra can be shown that $k' = 0$ and $kN_B^0 = k''$. These conditions for the constant rates can be easily obtained by using $\tau_1 = \tau_2$ in equation (2.30). There is no dissociation of the reversible bound complexes, and all bindings terminate as irreversible bindings. Obviously the decay is a single exponential one at rate $1/\tau$.

The amplitudes a and b in the solution for equation (2.10) can be determined from the initial conditions t=0 applied to equation (2.14) $N_{BP}^0 = a + b = 0$ and using equation (2.8) $\left.\frac{dN_{BP}}{dt}\right|_{t=0} = -\frac{a}{\tau_1} - \frac{b}{\tau_2} = kN_B^0 N_P^0$.

Therefore,

$$a = -b = \frac{kN_B^0 N_P^0}{\frac{1}{\tau_2} - \frac{1}{\tau_1}} \quad . \qquad (2.16)$$

Multiplying together equations (2.15) it can be shown that:

$$kk''\tau_1\tau_2 N_B^0 = 1 \quad . \qquad (2.17)$$

Therefore using equation (2.17) the constant a can take the alternative form: $a = \frac{N_P^0}{k''(\tau_1 - \tau_2)}$

Finally the solution of equation (2.10), describing the time evolution of transient bacterium-phage complexes is:

$$N_{BP}(t) = \frac{kN_B^0 N_P^0}{\frac{1}{\tau_2} - \frac{1}{\tau_1}}\left[\exp\left(-t/\tau_1\right) - \exp\left(-t/\tau_2\right)\right] , \qquad (2.18)$$

or alternatively:

$$N_{BP}(t) = \frac{N_P^0}{k''(\tau_1 - \tau_2)}\left[\exp(-t/\tau_1) - \exp(-t/\tau_2)\right] .$$

Plotting $N_{BP}(t)$ in figure 2-2, one sees that initially the population of transient bacterium-phage complexes increases with time with a rate determined by τ_1 and reaches a maximum N_{BPmax} at t_{max}, then decreases at late time with a rate determined by τ_2.

Note that all the plots in this section were calculated using the values we obtained from our experiments:

- initial bacterial population $N_{B0}=10^8 cm^{-3}$,
- initial free phage population $N_{P0}=10^5 cm^{-3}$,
- adsorption rate $k=2\cdot10^{-11} cm^3/s$,
- desorption rate $k'=3\cdot10^{-3} s^{-1}$,
- irreversible binding rate $k''=10^{-3} s^{-1}$.

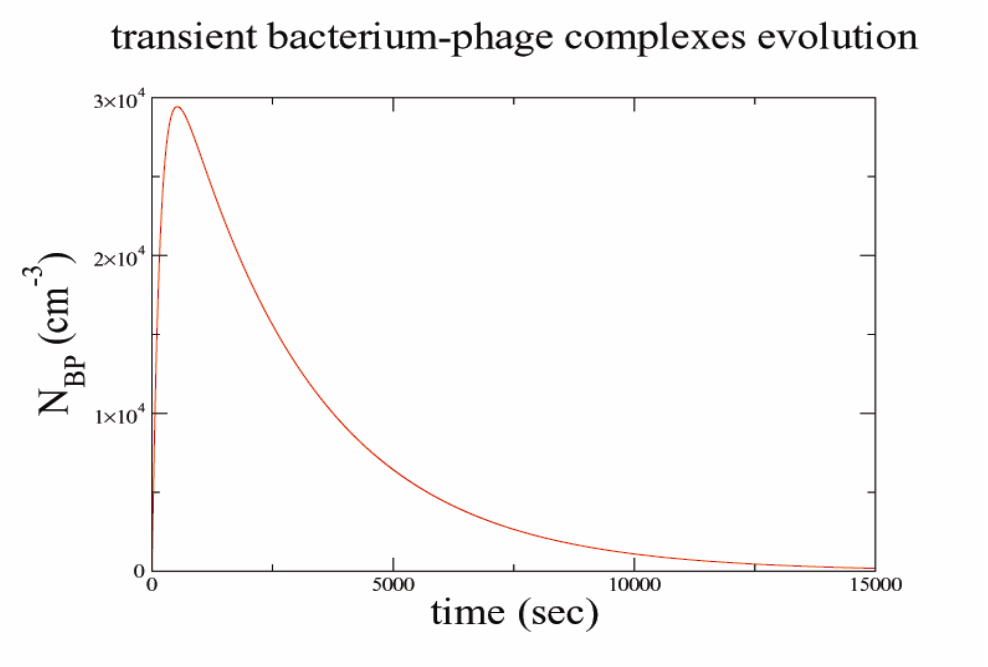

Figure 2-2 Transient bacterium-phage complex population evolving in time during the adsorption experiment

The expressions for the maximum population of complexes and for the time this maximum is reached are:

$$N_{BP\max} = kN_B^0 N_P^0 \tau_2 \left(\frac{\tau_1}{\tau_2}\right)^{\frac{\tau_2}{\tau_2-\tau_1}} \qquad (2.19)$$

$$t_{\max} = \frac{\tau_1\tau_2}{\tau_1-\tau_2}\ln\frac{\tau_1}{\tau_2}\ . \qquad (2.20)$$

Obviously there are no transient bacterium-phage complexes initially, and if there is a sink ($k'' \neq 0$), there are no transient bacterium-phage complexes after very long time as well $N_{BP}(\infty) \to 0$, as one can see from figure 2-2. When irreversible binding ($k'' \to 0$) is blocked, there is no sink for transient bacterium-phage complexes ($\tau_2 \to \infty$). Therefore the peak of the maximum disappears and equilibrium is reached, as seen in figure 2-3.

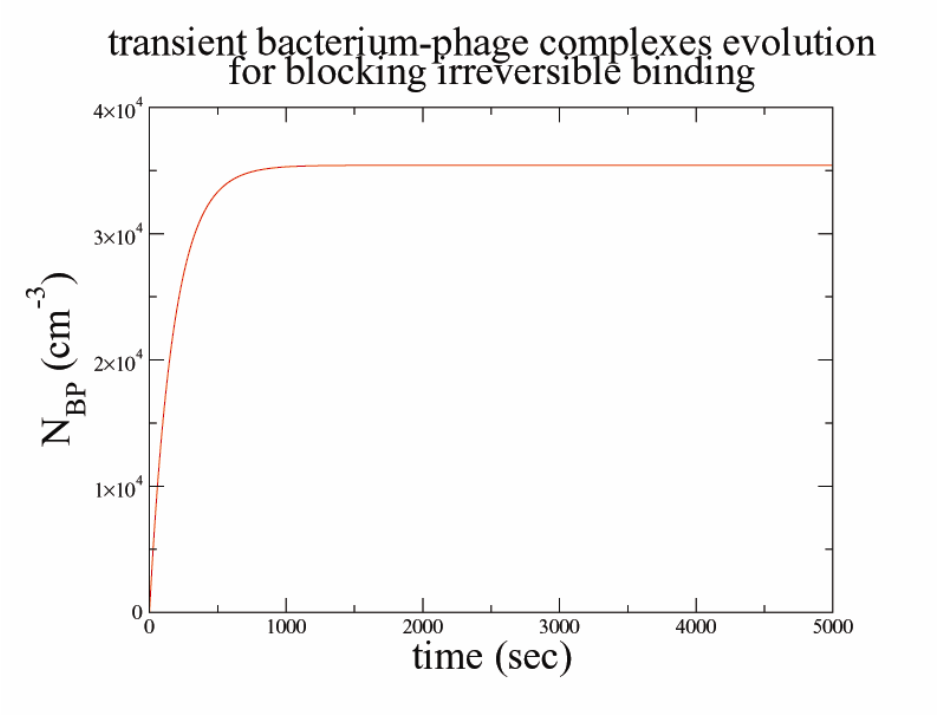

Figure 2-3 Transient bacterium-phage complex population evolving in time during the adsorption experiment for the case when irreversible binding is blocked

Here are the expressions for the limiting case where there is no phage sink:

$$N_{BP} \xrightarrow{k''=0} kN_B^0 N_P^0 \tau_1 \left[1-\exp\left(-t/\tau_1\right)\right]$$
$$N_{BP} \xrightarrow{k''=0,\ t\to\infty} kN_B^0 N_P^0 \tau_1 \quad . \tag{2.21}$$

In a similar fashion, one can calculate the evolution of infected bacteria population, or more precisely of permanent bacterium-phage complexes, by integrating equation (2.4). This yields:

$$N_{BP}^*(t) = \frac{N_P^0}{\tau_1-\tau_2}\left\{\tau_1\left[1-\exp\left(-t/\tau_1\right)\right]-\tau_2\left[1-\exp\left(-t/\tau_2\right)\right]\right\} \quad . \tag{2.22}$$

Clearly there are no infected bacteria initially. After very long time this population asymptotically tends to reach the initial phage population, which is expected for low MOI, i.e. the limit becomes

$$N_{BP}^* \xrightarrow{t\to\infty} \frac{N_P^0}{\tau_1-\tau_2}\cdot\left(\tau_1-\tau_2\right) = N_P^0 \tag{2.23}$$

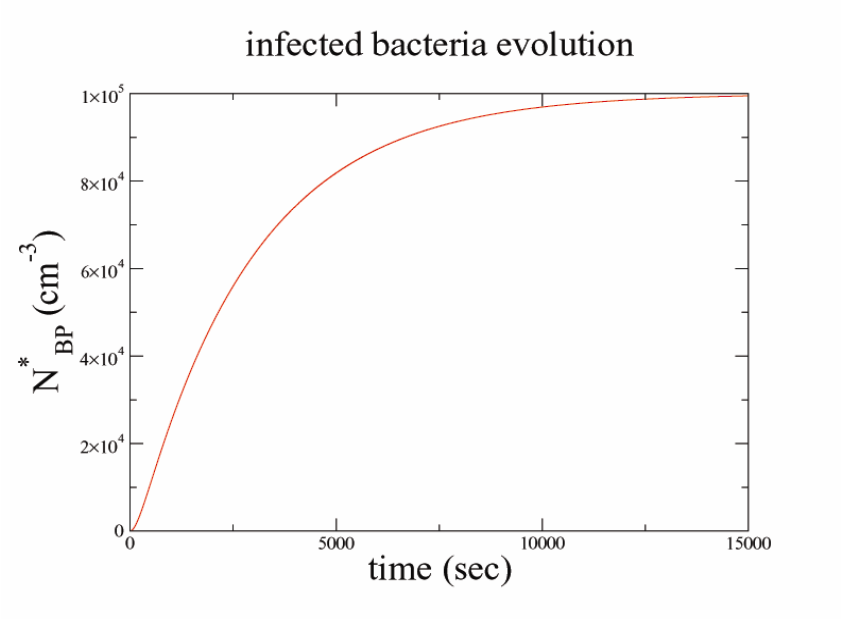

Figure 2-4 Infected bacteria population evolving in time during the adsorption experiment

Therefore infected bacteria population initially grows fast, and then eventually reaches equilibrium when all phages have infected cells, as seen in figure 2-4.

The observable in our experiment is the population of free phages. This is measured by standard titering methods. Recall equation (2.5) that states the conservation of the number of phages $N_P(t)=N_P^0-N_{BP}(t)-N_{BP}^*(t)$. After applying results for transient bacterium-phage complexes using equation (2.18) and for infected bacteria using equation (2.22), one can get the population of free phages normalized by its initial population:

$$\frac{N_P(t)}{N_P^0}=\frac{1}{\tau_1-\tau_2}\left[\left(\frac{1}{k''}-\tau_2\right)\exp\left(-t/\tau_2\right)-\left(\frac{1}{k''}-\tau_1\right)\exp\left(-t/\tau_1\right)\right]. \qquad (2.24)$$

As expected the free phages population is decaying in a two-exponential fashion (see figure 2-5). The short time decay is mainly determined by the adsorption rate k. The position of the "knee" of the plot is determined by the desorption rate k'. The long time decay is mainly determined by the irreversible binding rate k".

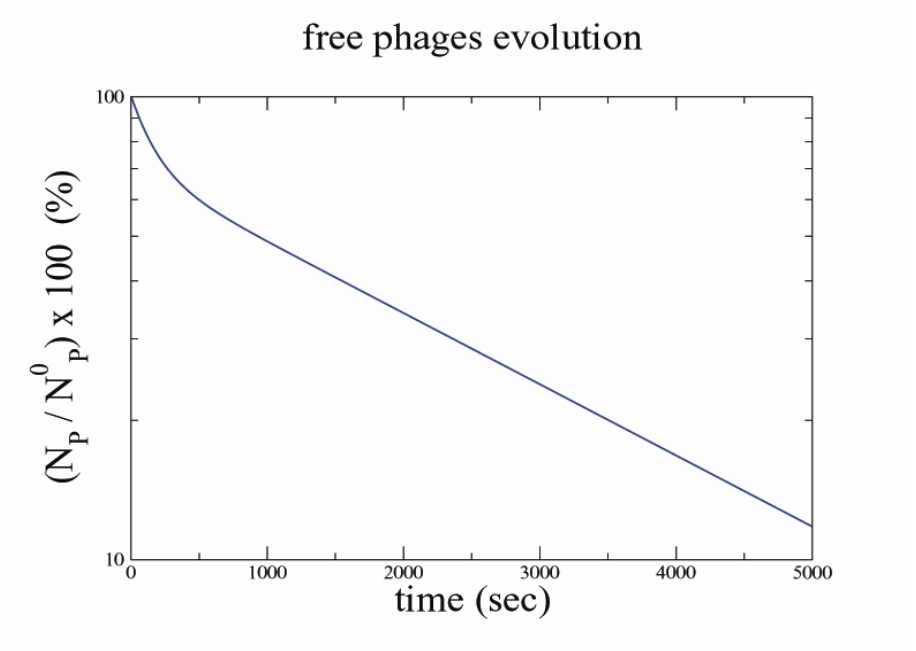

Figure 2-5 Free phages population evolving in time during the adsorption

The two exponential decay prediction for free phage population, equation (2.24), can be written in terms of three fitting parameters A, τ_1 and τ_2,

$$\frac{N_P(t)}{N_P^0} = A \cdot \exp\left(-t/\tau_2\right) + \left(1-A\right) \cdot \exp\left(-t/\tau_1\right) \ , \tag{2.25}$$

where $A = \dfrac{\dfrac{1}{k''} - \tau_2}{\tau_1 - \tau_2}$. (2.26)

There is a relationship between the three rate constants describing the adsorption process and the three fitting parameters A, τ_1 and τ_2. The easiest constant rate to obtain is the irreversible binding rate k" from the definition of A, equation (2.26). Therefore,

$$k'' = \frac{1}{A\left(\tau_1 - \tau_2\right) + \tau_2} \ . \tag{2.27}$$

Then, using equation (2.17) one can get the adsorption rate k as:

$$k = \frac{1}{k'' N_B^0 \tau_1 \tau_2} \ . \tag{2.28}$$

Let us introduce here the adsorption time $\tau_a = 1/kN_B^0$. Therefore,

$$\tau_a = k''\tau_1\tau_2 \ . \tag{2.29}$$

Finally, the desorption rate k' can be obtained by adding the two equations (2.15),

$$k' = \frac{1}{\tau_1} + \frac{1}{\tau_2} - N_B^0 k - k'' \ . \tag{2.30}$$

The advantage of our adsorption model consists in providing the three constant rates k, k' and k" by fitting parameters A, τ_1 and τ_2 in a single measurement. Adding and multiplying together the two equations in (2.15), one can obtain the folowing:

$$\tau_1 + \tau_2 = \tau_a + \frac{k'\tau_a + 1}{k''}$$

$$\tau_1 \cdot \tau_2 = \frac{\tau_a}{k''}$$

with solutions:

$$\tau_1 = \frac{1}{2}\left[\tau_a + \frac{k'\tau_a + 1}{k''} - \sqrt{\left(\tau_a + \frac{k'\tau_a + 1}{k''} \right)^2 - 4\frac{\tau_a}{k''}} \right], \tag{2.31}$$

$$\tau_2 = \frac{1}{2}\left[\tau_a + \frac{k'\tau_a + 1}{k''} + \sqrt{\left(\tau_a + \frac{k'\tau_a + 1}{k''} \right)^2 - 4\frac{\tau_a}{k''}} \right]. \tag{2.32}$$

Let us check if the dynamical equation (2.24) describing the evolution of free phages makes physical sense for several limiting cases:

i) In the case of a weak sink: $k'' << N_B^0 k, k'$, the two decay times τ_1 and τ_2 are:

$$\begin{aligned} \tau_1 &= \frac{\tau_a}{k'\tau_a + 1} \\ \tau_2 &= \frac{k'\tau_a + 1}{k''} \end{aligned} \quad . \tag{2.33}$$

Then equation (2.24) becomes:

$$\frac{N_P(t)}{N_P^0} = \frac{1}{1 + k'\tau_a} \exp\left(-t/\tau_1\right) + \frac{k'\tau_a}{1 + k'\tau_a} \exp\left(-t/\tau_2\right) . \tag{2.34}$$

For $k''=0$ $(1/\tau_2 = 0)$, the second exponential becomes unity and therefore the free phages population decays exponentially with the equilibrium reached at long time as expected, as seen in figure 2-6,

$$\frac{N_P(t)}{N_P^0} = \frac{k'\tau_a}{1 + k'\tau_a} + \frac{1}{1 + k'\tau_a} \exp\left(-\frac{1 + k'\tau_a}{\tau_a} t \right) . \tag{2.35}$$

Note that for t=0, the phage concentration ratio $N_P(0)/N_P^0 = 1$, as it should, and for t very long, $\frac{N_P(\infty)}{N_P^0} = \frac{k'\tau_a}{1+k'\tau_a}$.

The reaction equilibrium constant K_a can be determined by using equations (2.21), (2.34) and knowing MOI is low, meaning $N_B^\infty = N_B^0$. Therefore, $K_a = N_{BP}^\infty / N_B^\infty N_P^\infty = k/k'$ for blocked irreversible binding k"=0. Otherwise, for $k" \neq 0$ the long time equilibrium consists of $N_{BP}^\infty = 0$, $N_P^\infty = 0$ and $N_B^\infty = N_P^0$, which means no free phages, no transient complexes, and each phage infected a single bacterium.

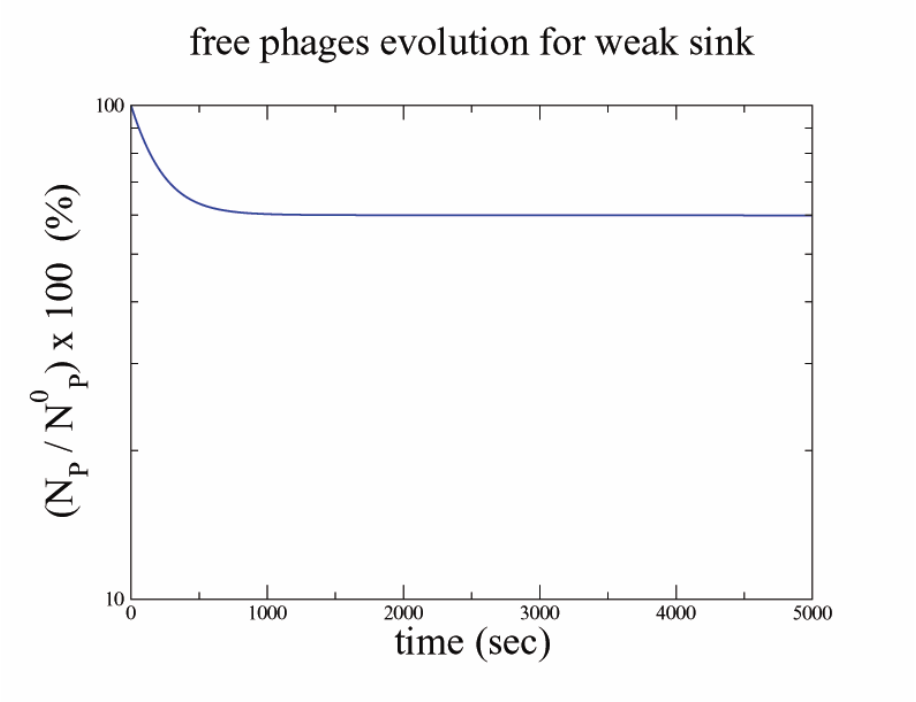

Figure 2-6 Free phages population evolving in time during the adsorption experiment for the case of blocked irreversible binding

ii) In the case of a strong sink limit: $k" >> N_B^0 k, k'$

$$\tau_1 = \frac{1}{k"} \quad . \qquad (2.36)$$
$$\tau_2 = \tau_a$$

Then equation (2.24) becomes:

$$\frac{N_P(t)}{N_P^0} = \exp\left(-t/\tau_a\right) , \qquad (2.37)$$

which is single exponential decay due to adsorption only, showing that desorption is insignificant.

Therefore in the case of a strong phage sink, adsorption leads immediately to irreversible binding for every single phage. Note that the adsorption rate, or more precisely $\tau_a^{-1}=N_B^0 k$, is the rate limiting step during the infection process and the population of transient bacterium-phage complexes N_{BP} is essentially zero at all time.

2.3 EXPERIMENTAL RESULTS

The observable in our experiments is the free phage population. We measure the concentration of free phages in time during the adsorption experiment by using a standard titering technique (for a detailed description of agar overlay technique, refer to Materials and Methods in Appendix). The curves in the figure 2-7 show the experimental data for the adsorption of lambda phages onto Ymel bacteria, which is an *E. coli* strain mainly used as indicator bacteria for titering lambda phages. There are four curves for four different temperatures. All of them show double exponential features, being nicely fit by our double exponential model. The fits are represented by continuous lines, while the experimental data is represented by symbols.

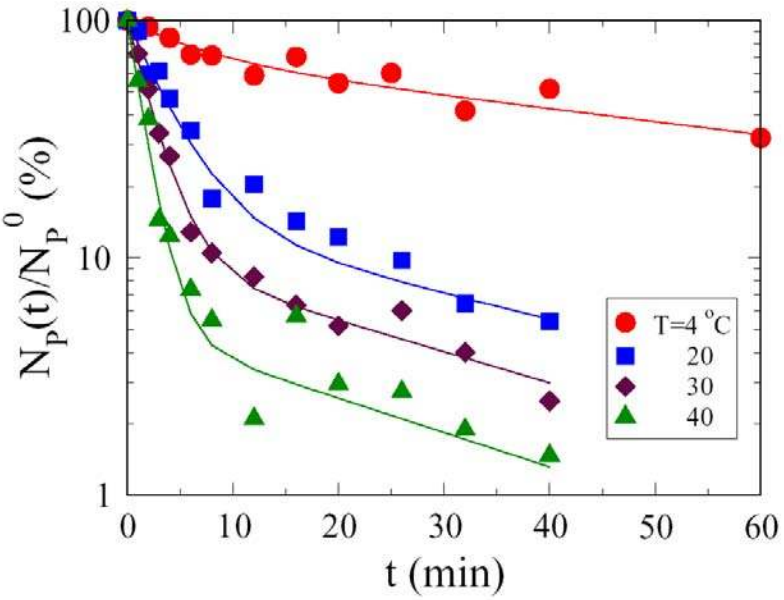

Figure 2-7 Adsorption curves data for 4 different temperatures

We used the software Origin 7 for fitting. First we fit the adsorption curves (plotted along with error bars due to counting statistics which is poissonian, therefore the standard deviation is square root of the mean) and get the three fitting parameters A, τ_1 and τ_2 with their uncertainties, as one can see in figure 2-8.

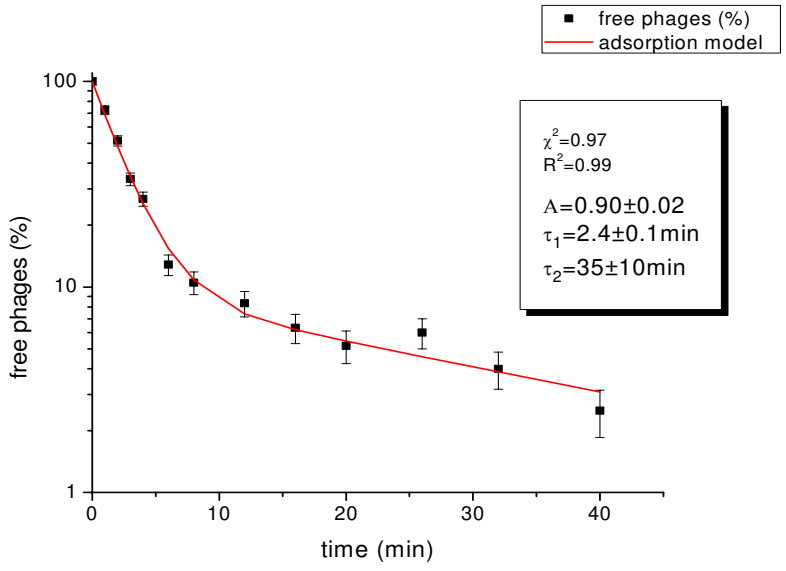

Figure 2-8 Obtaining the three fitting parameters A, τ_1 and τ_2 with their uncertainties

Then using equations (2.27), (2.28) and (2.30) we obtained the three rate constants k, k' and k" with their uncertainties by propagating the errors. Therefore plots of adsorption rate k, desorption rate k' and irreversible binding rate k" versus temperature are obtained, as can be seen in figures 2-9 and 2-10.

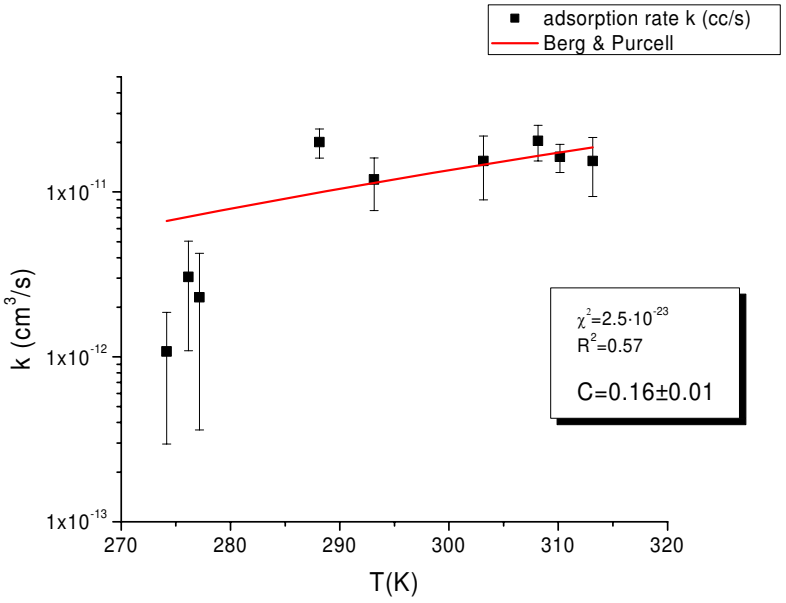

Figure 2-9 Adsorption rate vs. temperature fit by Berg & Purcell model

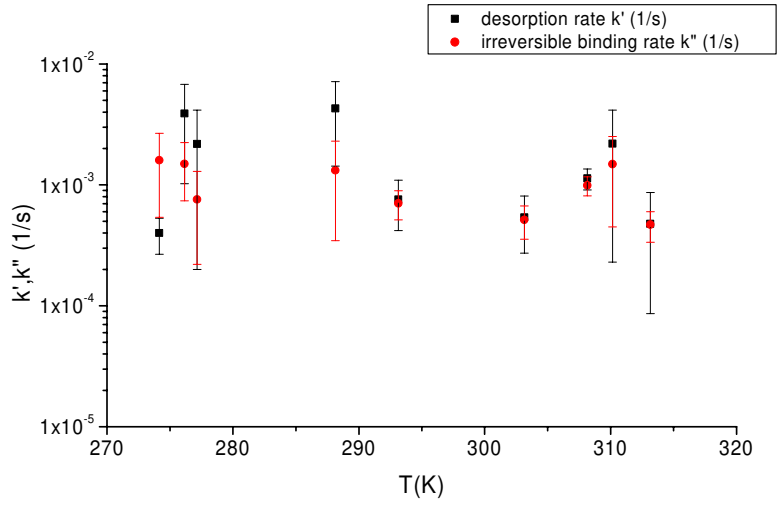

Figure 2-10 Desorption rate and irreversible binding rate vs. temperature

The reason for having uneven error bars for the plots of the rate constants versus temperature is the fact some adsorption curves were better fitted by our model than others. The aim of the fitting procedure is to find those values of the parameters which best describe the data. The standard way of defining the best fit is to choose the values for parameters p_1, p_2, … p_p, such that the sum (named chi square) of the squares of the deviations of the theoretical curve from the experimental points $\chi^2(p_1, p_2, ...) = \frac{1}{n^{eff} - p} \sum_i w_i [y_i - f(x_i; p_1, p_2, ...)]^2$ is minimum. Here, n^{eff} is the total number of experimental points used in the fitting, p is total number of adjustable parameters used in the fitting (the difference $n^{eff} - p$ is usually referred to as the number of degrees of freedom), w_i represent the weights of each experimental point, y_i are the experimental values, and $f(x_i;p_1, p_2,…)$ are the theoretical values. In all the fitting curves presented in this thesis the chi square value is obtained in Origin 7, as presented above, and is written in a box in the figure, along with another standard statistical quantity R^2. This is the coefficient of determination, which measures how well the regression line represents the data. If the regression line passes exactly through every point on the scatter plot, it would be able to explain all of the variation. The further the line is away from the points, the less it is able to explain. Its value ranges between 0 and 1, for the worst and the best fit, respectively.

2.3.1 Adsorption rate and number of receptors per cell

There clearly is a trend for the adsorption rate vs. temperature (see figure 2-9). We tried to use the Berg and Purcell adsorption model, equation 1.12, to fit our data and obtain the correction factor C for adsorption. First we obtained the two fitting parameters η_0 and E_a

(activation energy) from our viscosity measurements (see figure 2-11) for the buffer (10mM $MgSO_4$) in which we perform the adsorption measurements:

$$\eta = \eta_0 \exp\left(\frac{E_a}{k_B T}\right) . \qquad (2.38)$$

The reason of writing viscosity as an exponential function of activation energy (Arrhenius form) follows here (Glasstone, Laidler et al. 1941). The viscosity of a liquid is a measure of momentum transfer between molecules. In order to flow, the liquid molecules have to squeeze past their neighbors, transferring their momentum. For that they need to overcome an energy barrier, named activation energy E_a.

Using the Stokes-Einstein relation, equation (1.3), the diffusion coefficient D for the lambda phage particle can be written as a non-trivial function of temperature, equation (2.39).

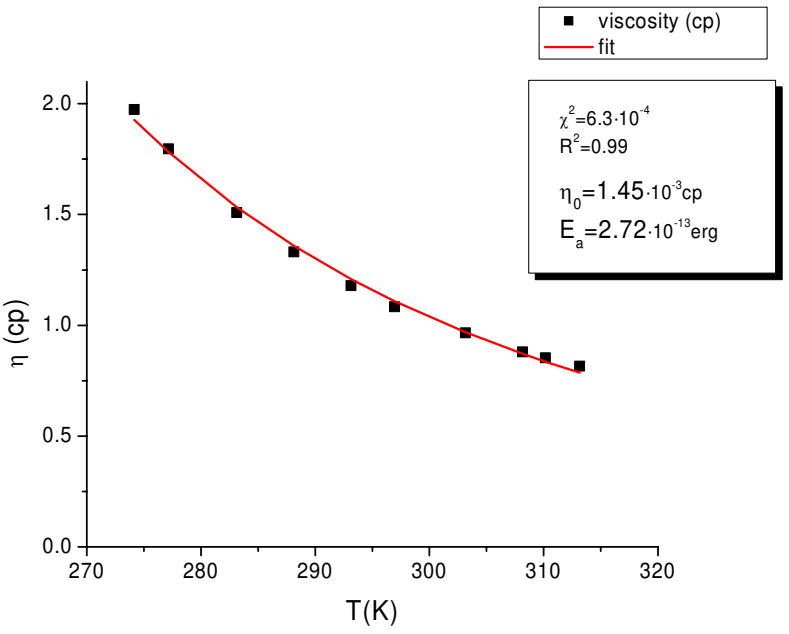

Figure 2-11 Viscosity of the adsorption buffer vs. temperature

$$D = \frac{k_B T}{6\pi R \cdot \eta_0 \exp\left(\frac{E_a}{k_B T}\right)} \quad . \qquad (2.39)$$

Therefore, the adsorption rate dependence on temperature based on Berg and Purcell model equation (1.12) and modified for the elliptical cells ($k_{\max} = 4\pi aD/\ln(2a/b)$ and $C \equiv \frac{Ns}{Ns + \pi a/\ln(2a/b)}$) is of the following form:

$$k = \frac{4\pi a}{\ln(2a/b)} \cdot \frac{k_B T}{6\pi R \cdot \eta_0 \exp\left(\frac{E_a}{k_B T}\right)} \cdot C \quad . \qquad (2.40)$$

Knowing cell size $a=1.9\cdot10^{-4} \pm .4$ cm from our measurements (refer to section 2.3.1.1 Cell length distribution), $\eta_0=1.45\cdot10^{-3}$cp, $E_a=2.72\cdot10^{-13}$erg from fitting in figure 2-11, and phage head radius $R=3\cdot10^{-6}$cm, we were able to fit our adsorption experiment data with equation (2.40) and obtained $C=.16\pm.02$ as seen in figure 2-9. One can get the number of receptors per cell, by using the modified definition of C for elliptical cells $N=\frac{\pi aC}{s(1-C)\cdot\ln(2a/b)}$, where the receptor size $s=4\cdot10^{-7}$cm. Therefore the number of receptors per cell for treating cells as ellipses is $N=142\pm21$. A similar estimation for the case when cells are considered spherical, by ignoring the logarithmic term, provides $N=132\pm21$.

Let us prove here that for a number of receptors per cell not very large the adsorption rate given by the Berg & Purcell model, as equation (1.12) states, is not affected whether the cell shape is spherical or ellipsoidal. The adsorption rate in equation (1.12) for an ellipsoidal cell would become:

$$k = \frac{4\pi aD}{\ln(2a/b)} \cdot \frac{Ns}{Ns + \frac{\pi a}{\ln(2a/b)}} \quad . \qquad (2.41)$$

One can see that for the case when $\pi a/\ln(2a/b) >> Ns$, the logarithmic term would cancel out and equation (2.41) becomes $k=4DNs$, which is the adsorption rate of N independent disks. In our case, $N=142$ receptors per cell, and indeed $\pi a/\ln(2a/b) \approx 3.0\cdot10^{-4}\text{cm} >> Ns \approx 5.6\cdot10^{-5}\text{cm}$. Considering the cells are spherical $\pi a \approx 6.3\cdot10^{-4}\text{cm} >> Ns \approx 5.2\cdot10^{-5}\text{cm}$, again πa cancels out in equation (2.41) and $k=4DNs$. Therefore for our cells it does not really matter whether we consider them spherical or ellipsoidal.

2.3.1.1 Cell length distribution

The cell size is important in most estimation of physical properties of bacterial strains. In figure 2-12 we present the cell length distribution of bacteria used in our adsorption experiments. The average value is $2a=3.9\pm0.7\mu m$; again a is the semi-major axis of the ellipsoid cell.

It is reasonable to assume that the cell size is linearly proportional to the number of the receptors $N=\alpha L$, where we introduce α to be the number of receptors per cell unit length. Therefore using the number of receptors per cell N obtained above and the average cell length one can determine the number of receptors per cell unit length $\alpha=36\pm9\mu m^{-1}$ or in other words how many receptors are on a micron length of cell. The error on α was determined by using a standard error propagation formula:

$$\frac{\sigma(\alpha)}{\alpha} = \sqrt{\left(\frac{\sigma(N)}{N}\right)^2 + \left(\frac{\sigma(L)}{L}\right)^2} \quad . \qquad (2.42)$$

The reason for using α rather than N will be discussed at the end of chapter 3.

We confirm this result experimentally by using fluorescence microscopy as can be seen in chapter 3.

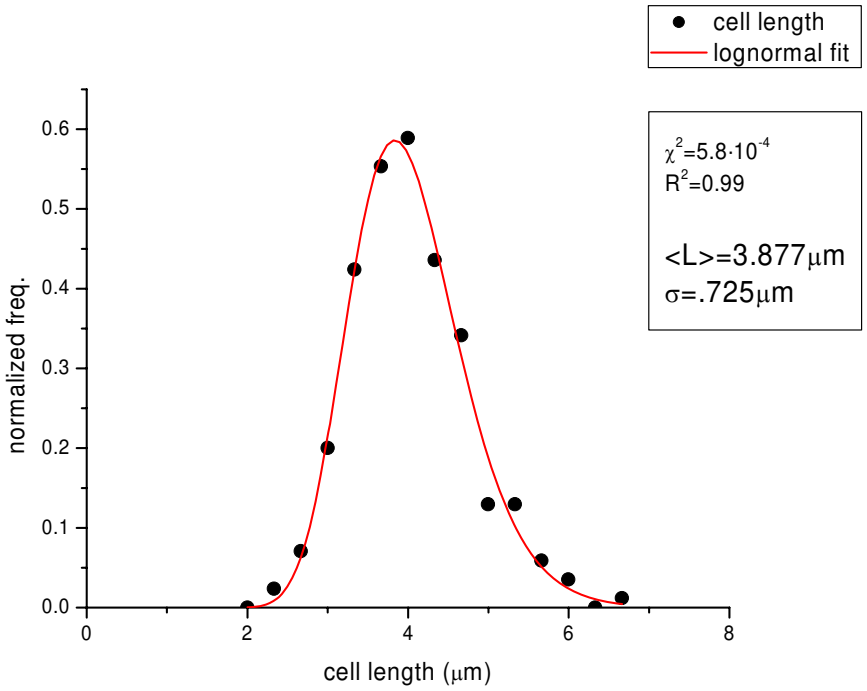

Figure 2-12 Cell length distribution for adsorption experiment

2.3.2 Dispersion of LamB receptors affected by low temperature

The low values for the adsorption rate at low temperature could suggest that receptors are not well distributed and tend to coagulate in patches as temperature decreases. Therefore the effective correction factor C^* for the case when the receptors coagulate in patches with decreasing temperature is of the following form:

$$C^* = \frac{Ms^*}{Ms^* + \pi a}, \qquad (2.43)$$

where M is the number of patches (containing multiple receptors) depending on temperature and s^* is the size of such a patch. Notice that here we don't bother to consider an elliptical shape for cells, since the difference in adsorption for elliptical cells vs. spherical cells is minor for low number of receptors per cell, as can be seen from equation (2.41). Let us introduce here the receptors coagulation coefficient $m=N/M$, and also mention that the size of a patch is related to the size of a single receptor as $s^*=s\cdot m^{1/2}$. Therefore,

$$C^*(m)=\frac{\frac{N}{\sqrt{m}}\cdot s}{\frac{N}{\sqrt{m}}\cdot s+\pi a} \quad . \qquad (2.44)$$

Notice the behavior of C^* at the extremes. For $m=1$, no coagulation, all receptors well dispersed and $C=C^*$. For maximum coagulation coefficient $m=N$, which means all receptors are grouped in one big patch:

$$C^*(m=N)=\frac{\sqrt{N}\cdot s}{\sqrt{N}\cdot s+\pi a} \quad . \qquad (2.45)$$

We do not know the mathematical form of the coagulation coefficient m dependence on temperature. But using equation (2.44) and our experimental data (see figure 2-9), we can determine its value for low temperature as follows. Since $\pi\cdot a$ is one order of magnitude larger than $N\cdot s$ ($6.3\cdot10^{-4}$cm>>$5.2\cdot10^{-5}$cm),

$$\frac{C^*}{C}=\frac{1+\frac{\pi a}{Ns}}{1+\frac{\pi a\sqrt{m}}{Ns}}\approx\frac{1}{\sqrt{m}} \quad . \qquad (2.46)$$

The ratio of the correction factors C^* and C equals the ratio of adsorption rates obtained for low temperatures where receptors are assumed to coagulate and adsorption rates obtained for room temperature where receptors are well dispersed. Using experimental data values one can

obtain the coagulation coefficient m≈60 for low temperatures and the number of patches, M=2.4. Therefore our experiment suggests that the receptors tend to group into two major patches when temperature lowers (see figure 2-13). This makes sense because cells usually keep their symmetry. Unfortunately, at this time, we do not have direct measurements, like fluorescent microscopy images showing the change in the receptors distribution with temperature, but we still can speculate the existence of sudden change in the distribution of receptors around 280K based on our adsorption experiment, as seen in figure 2-13.

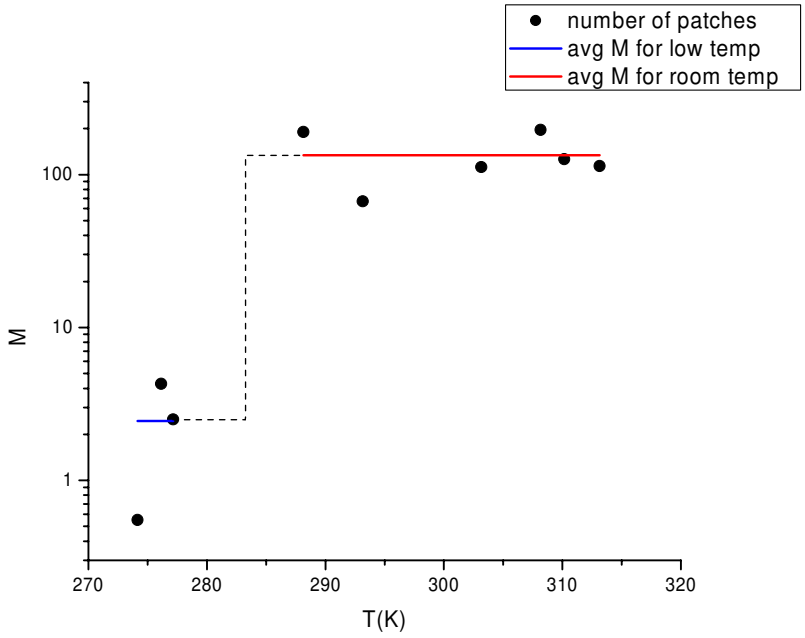

Figure 2-13 Variation of number of patches of receptors with temperature

2.3.3 Desorption rate and irreversible binding rate

The plots of desorption rate and irreversible binding rate, as seen in figure 2-10 show no dependence on temperature and seem to be of the same order of magnitude. A phage once adsorbed to the cell surface can either desorb or irreversibly bind. Since no temperature

dependence for desorption and irreversible binding rates appears, we believe these processes are entropic in nature. The rotational diffusion of the adsorbed phage helps in finding the right "key-lock" match that leads to irreversible binding. Therefore the rates can be written as:

$$k' = D_{rot} \cdot e^{-\frac{\Delta S'}{k_B}}$$
$$k'' = D_{rot} \cdot e^{-\frac{\Delta S''}{k_B}} \qquad (2.47)$$

where D_{rot} is the rotational diffusion coefficient of the phage along its long axis and $\Delta S'$, $\Delta S''$ are the entropy changes for the two states. Since the entropy is proportional to the state probability $S \sim -k_B \ln P$, one can write the ratio of the two rates as the ratio of the two corresponding probabilities (P' - probability of desorption and P'' - probability of irreversible binding):

$$\frac{k'}{k''} = \frac{D_{rot} \cdot e^{-\frac{\Delta S'}{k_B}}}{D_{rot} \cdot e^{-\frac{\Delta S''}{k_B}}} = e^{\ln P' - \ln P''} = \frac{P'}{P''} = \frac{P'}{1 - P'} \ . \qquad (2.48)$$

Once the phage adsorb onto bacteria, either desorb or irreversible bind, which makes the probability to be conserved. Since, the desorption rate in our experiments is ~2.3 times higher than the irreversible binding rate, the probability of an adsorbed phage to desorb is ~2.3 times higher than the probability to irreversibly bind. In order to figure out the entropic barrier for the two processes one has to estimate first the rotational diffusion constant. Therefore

$$D_{rot} = \frac{k_B T}{8\pi\eta R^3} \cong 4.9 \cdot 10^3 s^{-1} \ , \qquad (2.49)$$

from which it follows:

$$\Delta S' = -k_B \cdot \ln \frac{k'}{D_{rot}} \cong 14.9 k_B$$
$$\Delta S'' = -k_B \cdot \ln \frac{k''}{D_{rot}} \cong 15.7 k_B \ . \qquad (2.50)$$

It has been speculated that the interaction between lambda phage tail fiber and LamB receptor relies on a lock-key mechanism. Deleting or altering crucial sites on the receptors (see the green sites in figure 1-3) leads to an increase in the entropic barrier, hindering the completion of the infection process (Werts, Michel et al. 1994).

2.3.4 Adsorption of Ur-λ

We were able to obtain Ur-lambda phage from Hendrix lab in the Department of Biological Sciences, University of Pittsburgh (Hendrix and Duda 1992). The special feature of this lambda phage, which actually was the original isolate of lambda, is the extra appendages it possesses. The very thin three-segment angular fibers extend from the sides of the conical tip of the tail. These 4 tail fibers seem to help in adsorption onto cell membrane as one can see in figure 2-14.

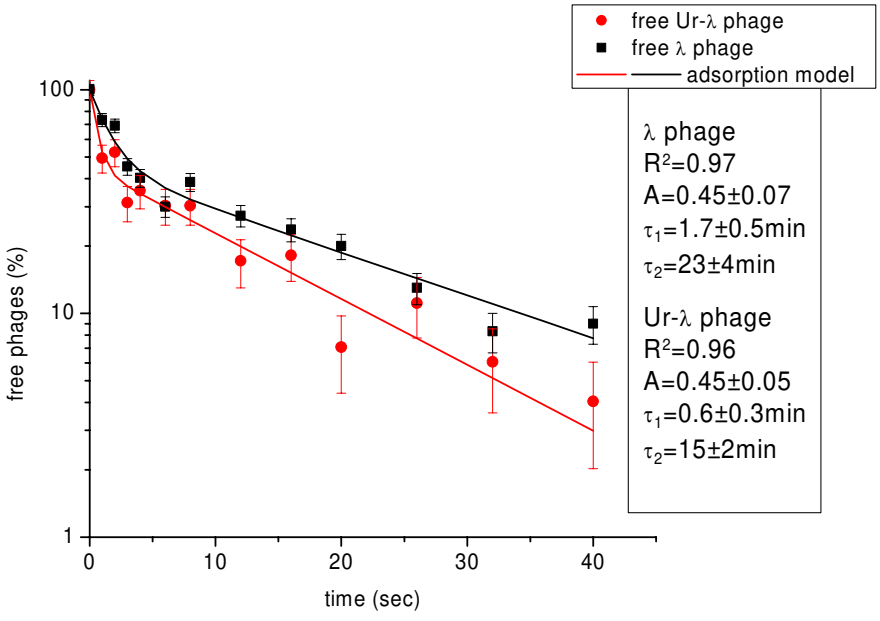

Figure 2-14 Adsorption of Ur-lambda vs. lambda

This results are in agreement with previous adsorption measurements of Ur-lambda performed in Hendrix lab (Hendrix and Duda 1992) and imply that the tail fibers of Ur-lambda are able to adsorb through a non-LamB receptor that is present on the surface of the cell. While both Ur-lambda and wild type lambda possess the gpJ tail fiber, which is responsible for LamB receptor recognition, only Ur-lambda has the extra appendages which make the desorption rate slower and increase the irreversible binding rate. Although we did not identify the non-LamB receptor on the cell surface responsible for enhancing the adsorption in the case of Ur-lambda, there is evidence suggesting that the OmpC membrane protein is recognized by the extra tail fibers (Montag, Schwartz et al. 1989).

2.3.5 Control experiment for conservation of phage number

Since our observable in the adsorption experiment is the concentration of free phages, we have to prove that phages are not disappearing during the adsorption experiment by other means than adsorption to cell membrane. In other words, the only sink for phages is the bacterial receptors, as stated in the adsorption model. Therefore a more complete experiment was carried in which not only unbound phages are titered, but bacterium-phage complexes as well. Data is presented in figure 2-15 and shows that the phage number is conserved during the adsorption experiment (for the adsorption buffer in which our adsorption experiments were done).

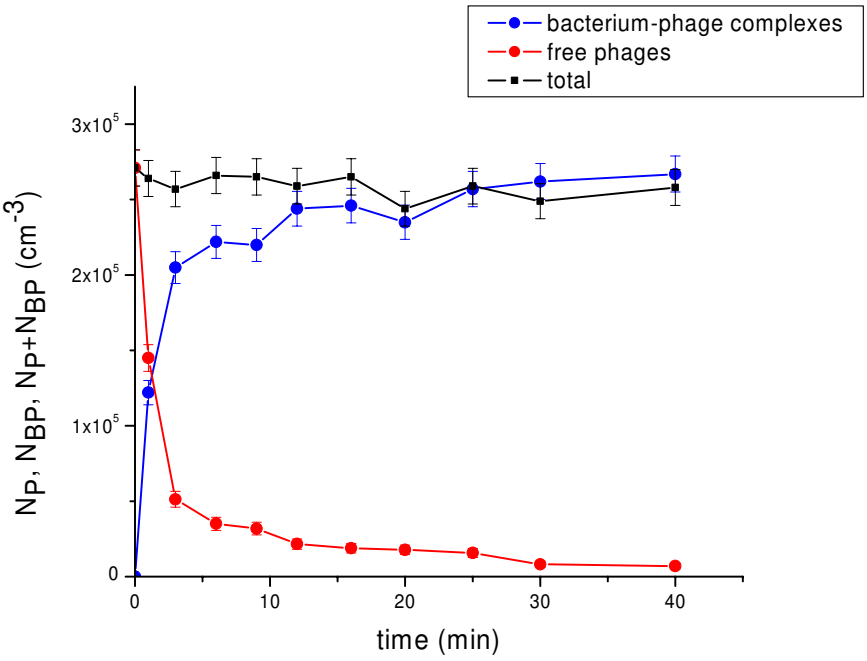

Figure 2-15 Control experiment showing conservation of phage number

2.4 CONCLUSIONS

We were able to develop a simple kinetics model which allows us to obtain the three rate constants k, k' and k" from a single measurement. Our experiment shows that the lambda phage adsorption is not anomalous. Its adsorption rate k is within the theoretical limit. We were able to estimate the number of receptors per cell by using our adsorption model along with Berg and Purcell model. Surprising features are revealed for k' and k". They are of the same order of magnitude; even though they are completely different processes. It seems there are only a few desorptions before irreversible binding.

3.0 QUANTIFICATION OF RECEPTORS

There is a strong urge to measure experimentally the number of receptors per bacterium in order to compare it to the theoretical estimation obtained by using our adsorption model together with the Berg and Purcell model.

We first wanted to use GFP labeled LamB receptors. However, GFP does not fold properly for fluorescence when exported from the cytoplasm via the general secretory pathway, therefore prohibiting its use for localizing outer membrane components (Feilmeier, Iseminger et al. 2000). Inspired by a previous work (Gibbs, Isaac et al. 2004), we attempted to use fluorescently labeled lambda phage tails. Unfortunately we never obtained satisfactory lambda phage tails with the concentration necessary for quantification of a high number of receptors per cell.

The next logical step would be to use fluorescently labeled phages. The disadvantage of using fluorescently labeled phages vs. using fluorescently labeled phage tails is the underestimation of the number of receptors due to the hindrance factor. This effect is sizeable only for the case of high number of receptors per cell. Considering the lambda phage head is ~60nm in diameter, the sectional area of the lambda phage head would be ~3000nm^2, that is ~.003μm^2. Therefore a cell of 12μm^2 surface area (a~2μm) would underestimate the number of receptors by using fluorescently labeled phages if there are more than 4000 receptors per cell.

There are two ways of obtaining fluorescently labeled phages. One way is by using Alexa Fluor 488 (carboxylic acid, succinimidyl ester, mixed isomers), a Molecular Probe dye product that label amine terminus of proteins and the ε-amino group of lysine. Alexa Fluor 488 is small (MW=643.41) compared to the lambda phage head, therefore there is no extra hindrance due to the dye. For a detailed description of the fluorescent labeling procedure see the Methods and Material chapter.

An alternative to the Alexa Fluor 488 labeling is the use of biotinylated phages coated with streptavidin and then conjugated with fluorescent biotin. We obtained the biotinylated phages from Prof. Jurgen Stolz of Universitat Erlangen-Nurnberg, Germany (Stolz, Ludwig et al. 1998). In order to propagate these phages we used an amplification protocol named PDS (pick, dilute, streak), which can be found in the Materials and Methods in the Appendix. The biotinylated phages possess a biotinylation domain linked to each gpD molecule, increasing its size from ~10kDa to ~30kDa. Also, streptavidin is a big tetrameric protein ($4*13$kDa). Therefore the increase in sectional area of the biotinylated phage head coated with streptavidin and then decorated with fluorescent biotin will be noticeable. A rough estimation using the average density of protein ρ=1.42g/cm^3 (Fischer, Polikarpov et al. 2004) would provide an extra 5.4nm layer relative to the wild type lambda phage. This will increase the sectional area by ~40% increasing the chance for underestimation of the number of receptors per cell. However the mixing of streptavidin with biotinylated lambda phages resulted in clusters of phages due to the multiple binding sites each streptavidin molecule has. Therefore we tried to skip the streptavidin coating step by growing the modified (biotinylation domain linked to gpD) lambda phage directly in fluorescent-biotin instead of regular biotin. Skipping the streptavidin coating step would not increase considerably the size of the labeled phage. The cells (strain Q358) used

for propagation of biotinylated phages are rich in birA, the enzyme responsible for biotinylation. Unfortunately we found that we could not label phages by direct exposure of the cells to the fluorescent-biotin. This can be due to two different things. One is the fact that the cells did not uptake the extracellular fluorescent-biotin molecules in order to decorate the biotinylation domain of the new crop of phages inside the cells. On the other hand one might ask the question if our biotinylated phages are indeed biotinylated, i.e. if they truly possess the biotinylation domain. In order to prove this we used a biotinylation detection kit (Phototope-Star from New England Biolab) to perform a western blot. The results surely indicated that we had biotinylated phages. The X-ray films, as can be seen in figure 3-1 clearly showed the biotinylated bands corresponding to the ~30kDa modified gpD (~20kDa biotinylation domain linked to ~10kDa gpD). For a description of the biotinylation detection method refer to the Materials and Methods in the Appendix. In order to overcome the inability of phage labeling by direct exposure of producing phage cells to fluorescent-biotin, one has to use in vitro biotinylation after the cell bursts in the presence of birA extract. Unfortunately the wild type birA is very inefficient for in vitro biotinylation. Although, there are mutants of birA reported to have a much higher efficiency (Choi-rhee, Schulman et al. 2004).

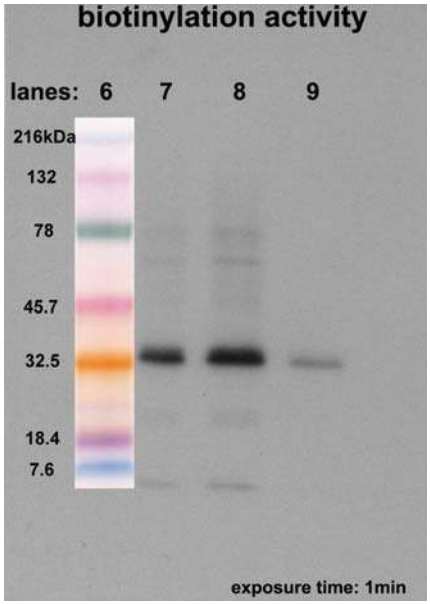

Figure 3-1 X-ray film showing biotinylation activity of the modified gpD

Because of the easiness and high efficiency of the reaction and because of the stability of the labeled product, we chose to use Alexa Fluor 488 for labeling lambda phages directly. Labeling lambda phages affects their infectivity by blocking crucial sites on gpJ, responsible for binding to LamB receptors. We searched for an optimal ratio of dye concentration to phage concentration such that the infectivity of phages is not considerably affected. We found by titering phages before and after labeling, that a three order magnitude difference between dye concentration and phage concentration would not affect the phage infectivity by more than 5%, which correspond to a concentration of 6.25μM of Alexa Fluor 488 for a phage concentration of $5 \cdot 10^{12} cm^{-3}$, as can be seen in figure 3-2.

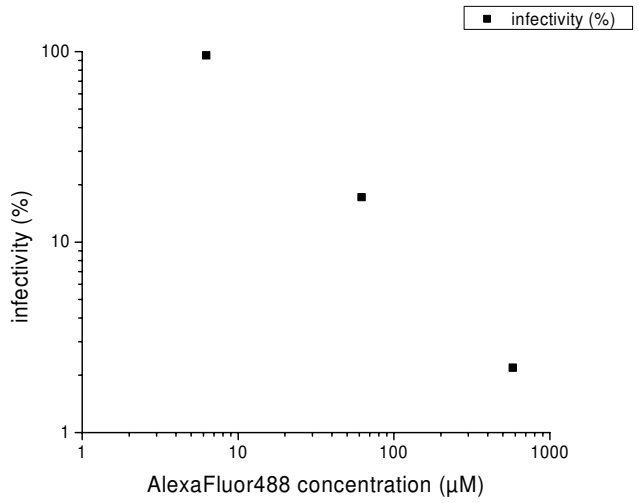

Figure 3-2 Infectivity of dye labeled phages

Using fluorescence microscopy, we obtained the probability density function of the fluorescently labeled phage brightness as can be seen in figure 3-3 for the ones labeled with 6.25μM dye. It seems the labeling process took place homogeneously, and a normal distribution can appropriately fit the PDF. We estimated the number of phages bound per cell by dividing the fluorescent intensity of the cell by the average value of the phage fluorescent intensity. Figure 3-4 shows individual fluorescent phages and ornate cells with attached fluorescent phages.

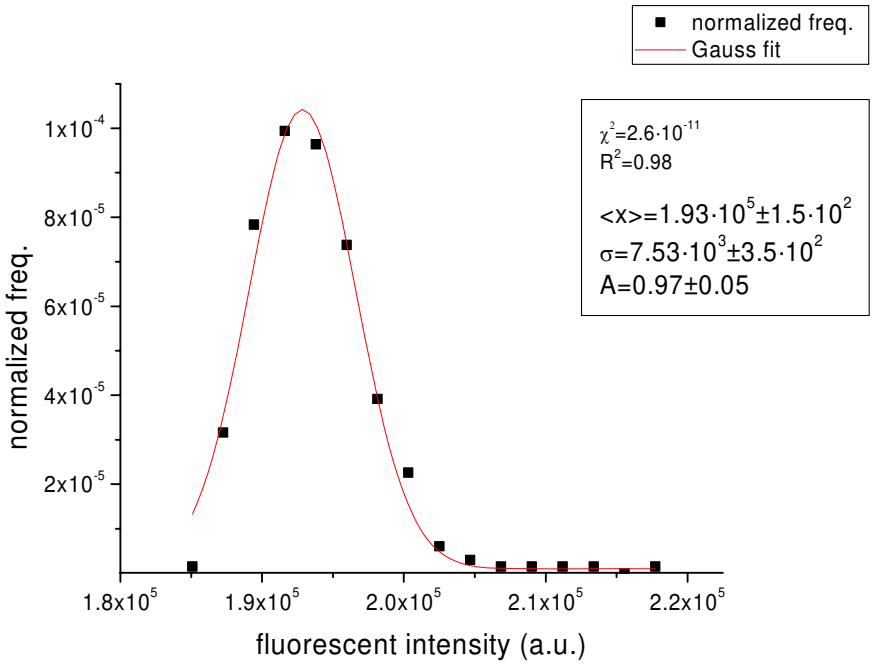

Figure 3-3 PDF of fluorescent labeled phage intensity

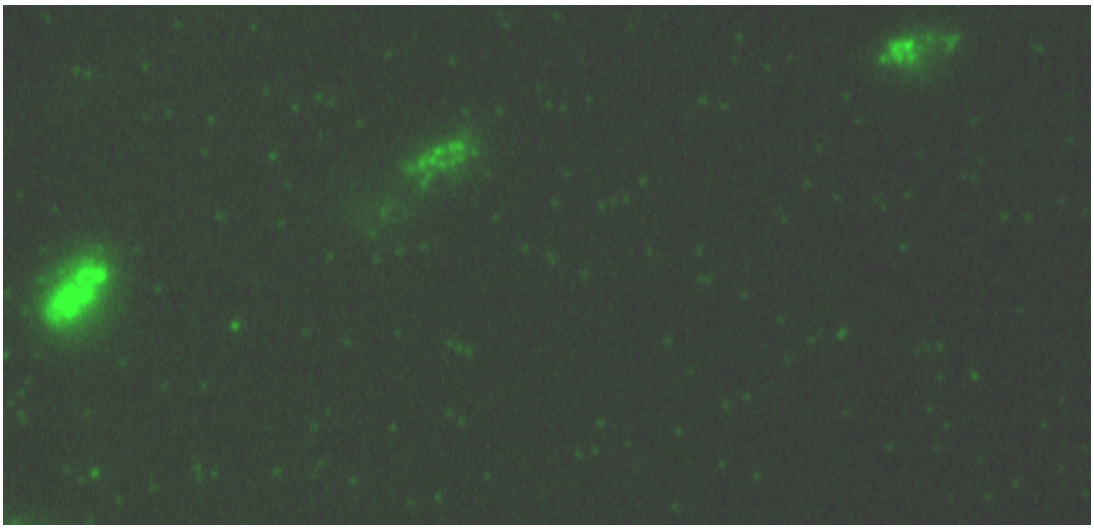

Figure 3-4 Fluorescent phages and cells

We set up four different reactions in which fluorescent phages were incubated with bacteria at four different MOI, for 70 min at 37°C. After stopping the reaction and washing free fluorescent phages away, fluorescent and phase pictures of cells glued to the cover slip were

taken. All the imaging acquisition and analysis was performed using the software SimplePCI, version 5.3.0.1102 coupled to a CCD camera, Hamamatsu model C9100-12. All fluorescent pictures for the four different experiments had the same exposure time (Δt=5s) and gain (gain=150). Each fluorescing cell was delimitated as a region of interest (ROI) before measuring its fluorescence intensity. After calibrating the fluorescent intensity of individual labeled phage (see figure 3-3) we estimate the number of phages bound to each cell. The experimental data representing the distribution of number of phages per cell for the four different MOI reactions allowed us to estimate the number of receptors per cell as follows.

Assuming each bacterium has N receptors, and each of them has a probability f to be bound to a phage, then the conditional probability that a cell with N receptors has n phages bound to it, is given by the binomial distribution:

$$P(n,N) = \frac{N!}{n!(N-n)!} \cdot f^n \cdot (1-f)^{N-n} \quad . \qquad (3.1)$$

Considering the phage flux to one receptor (disk of radius s) is $j_0 = 4DsN_p$ (Berg 1993) and $j_0 \cdot dt$ is the elementary probability that a receptor will be hit by a phage in a time dt, which we can choose short enough such that $j_0 \cdot dt << 1$ and Poisson statistics works. Using similar logic as we use for survival statistics discussion in section 4.4.1 The need of persisters, we get the probability for a receptor to be hit by phages, and therefore to be bound to a phage:

$$f(t) = 1 - e^{-j_0 \cdot t} \quad . \qquad (3.2)$$

The probability that a receptor is not occupied by a phage after a very long time t is essentially zero, as expected

$$1 - f = e^{-j_0 \cdot t} \xrightarrow{t \to \infty} 0 \quad . \qquad (3.3)$$

Actually not all cells have the same number of receptors; therefore more correctly:

$$P(n)=\sum_{N=n}^{N\max}P(n,N)\cdot Q(N)=\sum_{N=n}^{N\max}\frac{N!}{n!(N-n)!}\cdot f^{n}\cdot\left(1-f\right)^{N-n}\cdot Q(N)\ , \tag{3.4}$$

where Q(N) is the distribution of the number of receptors per cell. Notice that for n>N the factorial in the denominator is not defined, therefore the lower limit of number of receptors per cell is n, number of phages bound per cell, which makes perfect sense; it is necessary to have at least n receptors per cell in order to be able to bind n phages.

We assume that the cell size is linearly proportional to the number of the receptors per cell $N=\alpha L$. Recall α we introduced in section 2.3.1.1 Cell length distribution, which is the number of receptors per cell unit length. Therefore one can perform a transformation of cell length distribution R(L) into the number of receptors per cell distribution Q(N):

$$Q(N)dN=R(L)dL\Rightarrow Q(N)=\frac{dL}{dN}R(L)=\frac{1}{\alpha}R(L)\ . \tag{3.5}$$

We obtained the cell length distribution R(L) for each one of the four different reactions. Their averages seemed to slightly decrease due to the fact they were deprived (because of the washing) of nutrients and they kept dividing while waiting for their turn to be pictured and analyzed. The cell length distribution is lognormal fitted by (3.6), which is in agreement with previous reports (Furusawa, Suzuki et al. 2005). The cell length distributions for different reactions of different MOI are shown in figure 3-5.

$$R(L)=\frac{e^{-\frac{\left(\ln\frac{L-L_0}{m_L}\right)^2}{2\sigma_L^2}}}{\left(L-L_0\right)\sigma_L\sqrt{2\pi}}\ , \tag{3.6}$$

where L_0 is the cut off in cell length distribution, and m_L and σ_L are the average and the standard deviation for R(L), all known from fitting.

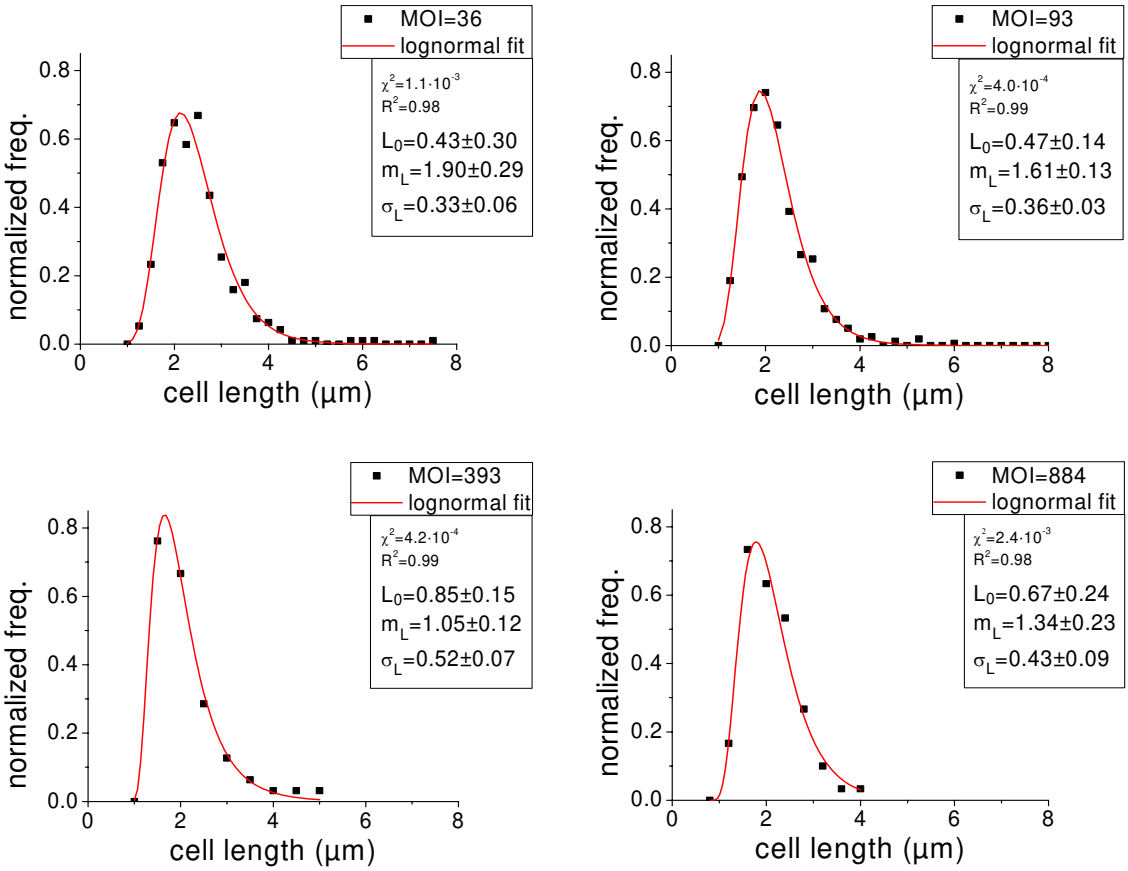

Figure 3-5 Cell length distribution for number of receptors quantification experiment

Then, using equation (3.5), Q(N) can be written as

$$Q(N) = \frac{1}{\alpha} \cdot \frac{e^{-\frac{\left(\ln\frac{L-L_0}{m_L}\right)^2}{2\sigma_L^2}}}{(L-L_0)\sigma_L\sqrt{2\pi}} \quad . \qquad (3.7)$$

Using $N=\alpha L$ and equation (3.7), the probability of having n phages bound to a cell with N receptors, described by the equation (3.4), becomes:

$$P(n)=\sum_{N=n}^{N\max}\frac{N!}{n!\cdot(N-n)!}\cdot f^{n}\cdot(1-f)^{N-n}\cdot\frac{1}{\alpha}\cdot\frac{e^{-\frac{\left(\ln\frac{\frac{N}{\alpha}-L_0}{m_L}\right)^2}{2\sigma_L^2}}}{\left(\frac{N}{\alpha}-L_0\right)\sigma_L\sqrt{2\pi}}\quad.\tag{3.8}$$

This is the distribution function we utilized to fit our fluorescent data. The number of receptors per cell unit length α and the probability of a receptor to be occupied by a phage f are obtained as fitting parameters. Figure 3-6 shows the fitting to our four data sets, corresponding to different MOI.

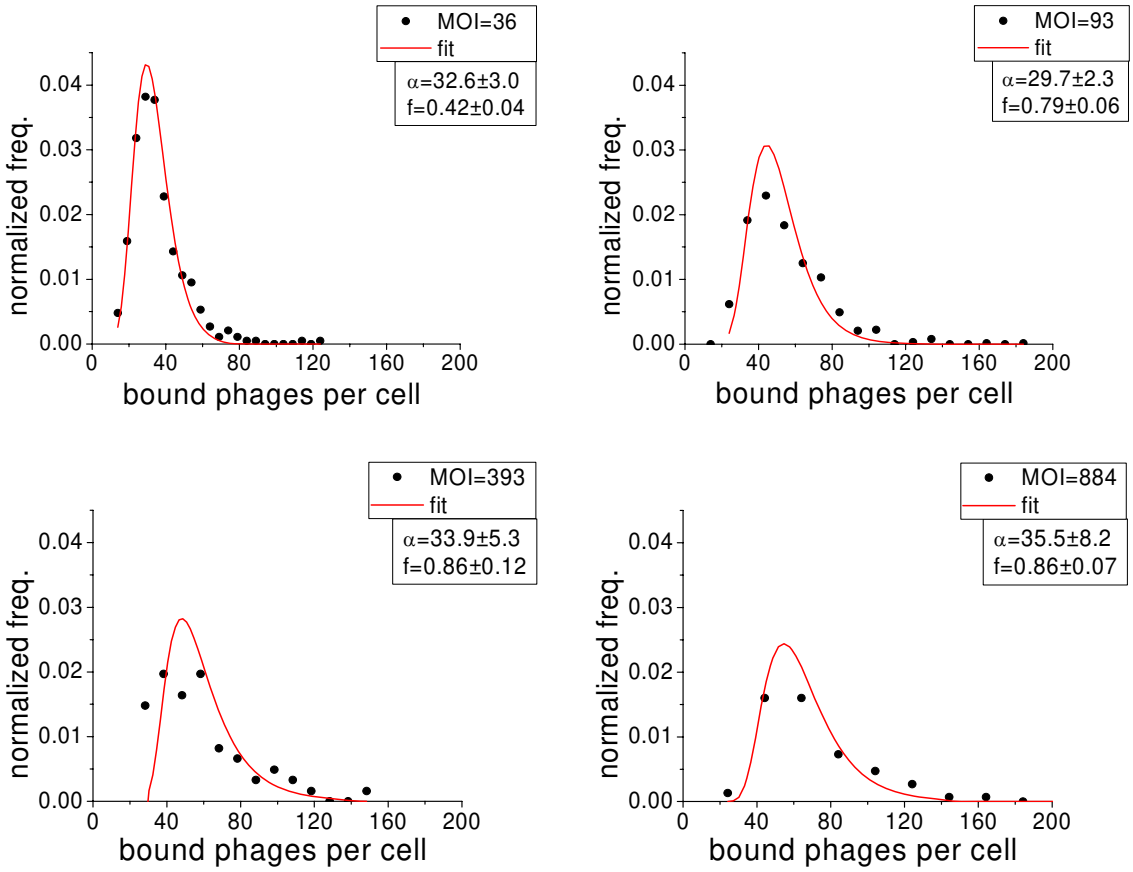

Figure 3-6 Bound phages per cell

The results of fluorescent imaging analysis are summarized in table 3-1. It contains the two fitting parameters. It was also added the column with theoretical values for f, the probability of occupation of a receptor by a phage for the reaction time of 70 minutes, calculated using equation (3.2) and the phages flux to a single receptor $j_0=4DsN_p$. Again, we utilized here $D=5\cdot10^{-8}cm^2/s$ as value of phage diffusion constant in 10mM $MgSO_4$ at 37°C and $s=4\cdot10^{-7}cm$ as radius of the receptor. The incubation time for bacteria and labeled phage reaction was $t=70$ min.

Table 3-1 Fluorescence imaging analysis results

MOI	N_B (cm^{-3})	N_P (cm^{-3})	experimental f	uncertainty f	theoretical f	α (μm^{-1})	uncertainty α
36.05	6.73E+07	2.43E+09	0.423	0.039	0.56	32.60	2.96
92.77	6.54E+07	6.07E+09	0.790	0.062	0.87	29.70	2.27
392.63	3.09E+07	1.21E+10	0.856	0.119	0.98	33.87	5.26
883.50	2.75E+07	2.43E+10	0.857	0.071	1.00	35.48	8.23

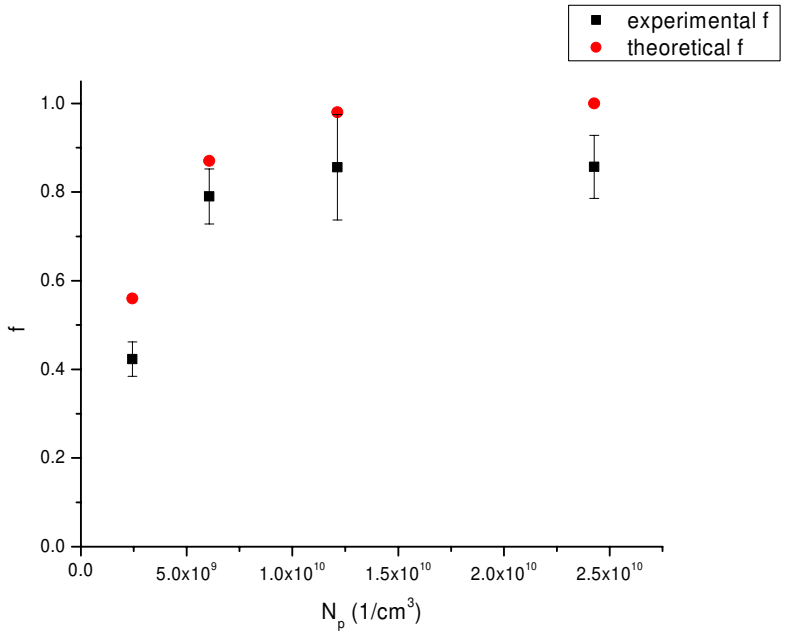

Figure 3-7 Probability f of receptor occupation by a phage

As it can be seen in figure 3-7, one of the fitting parameters, the experimental f is lower than the theoretical f. The reason may be the following. We calculate theoretical f using equation (3.2) where $j_0=4DsN_p$ and the receptor is assumed to be a perfect adsorber, which we know is not the case since there is desorption, slowing down the binding. Therefore a lower experimental f makes sense. For the other fitting parameter we obtained α=32.91±2.61 receptors per μm, cell unit length. The value for α is the average of α values obtained for the four different experiments and the error of α was obtained using propagation of errors $\sigma_\alpha = \frac{1}{4}\sqrt{\sum_{i=1}^{4}\sigma_{\alpha i}^2}$. The advantage of obtaining α, the number of receptors per μm, instead of obtaining N, the number of receptors per cell, is the following. We believe that LamB receptors expression level is constant for a certain cell strain in a given environmental condition (i.e. M9 media supplemented with glucose), while

the cell length may vary as growing condition is different (i.e. log phase vs. stationary phase). In other words, the receptors expression is an intrinsic feature while the length is not.

3.1 CONCLUSIONS

Comparison of the two values of α, one obtained in chapter 2 (paragraph 2.3.1) by our adsorption experiment with α=36±9, and one, by fluorescence microscopy with α=33±3, one can conclude that the agreement between the two methods is quite good. The latter method is more direct and perhaps more accurate, showing less uncertainty.

4.0 POPULATION DYNAMICS EXPERIMENT

The interaction between lambda phage and its host *E. coli* bacterium at the population level can be very spectacular. We also built a theoretical model to predict the evolution for the two populations. We performed population dynamics experiments to monitor the time evolution of the two populations. The dynamics of the two populations was observed in different growth media (i.e. minimal M9 media supplemented with glucose or maltose) during 30 hours long experiments. The initial conditions were varied such that different initial MOI were studied. Recall that MOI, multiplicity of infection = N_P/N_B is the ratio between the phage population and bacteria population.

A very striking feature of the population of bacteria was observed in the case of very high MOI. Even though the phages outnumbered the bacteria by a few orders of magnitude, the killing was not complete. Always there is a very small bacterial subpopulation surviving the massive phage attack. To date, there are no reports describing such surviving behavior to phage pressure. Although recently, similar surviving behavior to antibiotics pressure, but not to phage pressure, was reported (Balaban, Merrin et al. 2004; Kussell, Kishony et al. 2005). Persisters, by definition, can survive the phage attack, the antibiotics treatment or any other pressure, due to the state they are in, but after some time turn back into normal cells and become again vulnerable. Therefore there is a rate of switching of persisters into normal bacteria, and also there is a rate of switching of normal bacteria into persisters. We were able to obtain these rates for our bacteria.

Another feature of population dynamics experiment worth to be mention here is the fact that after long time interaction between bacteria and phages, they start to coexist peacefully as their concentrations become steady.

We do not claim here that persisters are the same for all types of pressure, or in other words that the persisters to phage attack would survive antibiotics treatment. Although, this universality of persistence might not be far from the reality, the work here does not deal with other pressure than phages. Yet, we encourage multiple pressure type studies leading to confirmation of persistence universality.

4.1 EXPERIMENTAL PROCEDURE

The population dynamics experiments were performed at 36°C. We started the incubation with a low MOI; therefore phages are outnumbered by bacteria. Every hour the incubation media is sampled out and bacteria are separated from phages by centrifugation. The concentration of the two competing population are obtained. Standard titering using agar overlay technique was performed in order to obtain the concentration of phages population. A detailed experimental protocol can be found in the Appendix: Materials and Methods. High initial MOI experiments, which we call killing experiments, were also performed.

4.2 POPULATION DYNAMICS MODEL

We tried to describe the complexity of the population dynamics by using the following set of differential equations. Note that the main difference between this set of differential equations and the adsorption model is the addition of production terms of bacteria and phages. One can see that the number conservation law is obeyed for all populations in the differential equations system; notice that the "source" terms (positive terms) and the "sink" terms (negative terms) are paired together.

$$\frac{dN_{BN}}{dt} = \left[\lambda_N \left(1 - \frac{N_{BN} + N_{BP}}{K} \right) - \gamma N_P \right] N_{BN} + \beta N_{BP} - \alpha N_{BN} \tag{4.1}$$

$$\frac{dN_{BP}}{dt} = \lambda_P \left(1 - \frac{N_{BN} + N_{BP}}{K} \right) N_{BP} - \beta N_{BP} + \alpha N_{BN} \tag{4.2}$$

$$\frac{dN_P}{dt} = m\varepsilon N^*_{BN} - \gamma \left(N_{BN} + N^*_{BN} + N_{BD} \right) N_P \tag{4.3}$$

$$\frac{dN^*_{BN}}{dt} = \gamma N_{BN} N_P - \varepsilon N^*_{BN} \tag{4.4}$$

$$\frac{dN_{BD}}{dt} = \varepsilon N^*_{BN} - \eta N_{BD} \ . \tag{4.5}$$

The dynamic variables are:

N_{BN}: Concentration of normal bacteria (pre-infection)

N_{BP}: Concentration of persisting bacteria (anytime)

N_P: Concentration of free phages (pre-infection)

N^*_{BN}: Concentration of phage-bacteria complexes (post-infection, pre-lysis)

N_{BD}: Equivalent concentration of bacterial debris (post-lysis)

The parameters are:

λ_N, λ_P: Growth rate for normal bacteria and persisting bacteria

γ: Adsorption rate of phages onto normal bacteria and debris

α: Switching rate from normal bacteria to persisting bacteria

β: Switching rate from persisting bacteria to normal bacteria

ε: Lysing rate for infected bacteria

m: Burst size (the new crop of phages produced by one cell)

η: Degradation rate for bacterial debris

The robustness of the model relies on the fact that the equilibrium conditions reached at the end of the run are the same for varied values of most of the parameters. It seems that the most sensitive parameters are m and η.

There are two types of populations: bacteria and phages. The bacterial population consists of two subpopulations: normal bacteria that get infected by phages and persisters that can survive phage attack. As can be seen in the first two differential equations, describing the evolution of the bacterial subpopulations N_{BN} (normal bacteria) and N_{BP} (persisting bacteria), there is a "source" term due to growing of bacteria and a "sink" term due to adsorption/infection by lambda phages in case of normal bacteria but not in the case of persisters which are resistant to lambda phage infection due to a lack of functional receptors. We have fluorescence images showing that persisters do not adsorb phages. There is another pair of "source" – "sink" terms corresponding to the switching rate between the two types of bacteria. Notice that the "source" and "sink" terms are switched for the two bacterial subpopulations in order to fulfill the number conservation law. Also, notice that the growing of bacterial population is limited by the logistic term with a carrying capacity K (Royama 1992). Based on our experimental data we used

$K=10^9 cm^{-3}$ for glucose supplemented M9 media and $K=5\cdot10^8 cm^{-3}$ for maltose supplemented M9 media.

In a similar fashion, the free phage population N_P (the third differential equation in our model) evolves according to a "source" term due to the production of a new crop of phages by the infected cells and again a "sink" term, here a triple term due to adsorption of phages onto normal bacteria (infected or not infected) and onto debris. The fourth differential equation in the model is describing the evolution of the infected bacteria (called also bacterium-phage complexes) with the "source" being adsorption/infection process while the "sink" is the bursting process. The last differential equation, describing the evolution of bacterial debris encloses the description of the population dynamics according to the number conservation principle.

Our model is based on real phenomena, experimental evidence being available in all aspects. All the processes: adsorption, infection, bursting and switching between normal and persisters are real facts which put together make the big picture of population dynamics model complete. The model must explain the experimental data for all different initial conditions. Our experimental observables were the concentration of total bacterial population N_B (normal bacteria and persisters) and the concentration of free phages population N_P. The model was solved numerically by using XPPAUT, software created by Prof. Bard Ermentrout (Univ. of Pittsburgh, Department of Mathematics). XPPAUT is a tool specialized in solving differential equations (http://www.math.pitt.edu/~bard/xpp/xpp.html). After obtaining the simulation in XPP we imported it into Origin 7.0 for displaying purpose.

4.3 RESULTS

Within our model, using the rate values (parameters) obtained in other experiments, we generate evolution curves for the two populations and compare with experimental data. The competing populations were studied in two different media: M9 supplemented with maltose and M9 supplemented with glucose at incubation temperature of 36±1°C for low initial MOI. Glucose supplemented M9 media cause bacteria to divide faster, therefore their size is smaller and the burst size (the new crop of phages produced by each cell) is also smaller comparing to the maltose supplemented M9 media case where the cells grow bigger in size.

4.3.1 Experimental data and simulation

In figure 4-1 we present experimental data for low initial MOI population dynamics experiments, performed in the two different media: maltose supplemented M9 media and glucose supplemented M9 media. Data is more spectacular in the case of maltose supplemented M9 media. Initially bacteria grew unaffected by the small phage population, but as soon as phages started to increase in population due to the phage infection and production, they would take over and decimate bacterial population. It seems even for such a huge MOI, which was reached around time 12 – 13 hours, not the whole bacteria got killed by the devastating phages. We believe this small subpopulation is a special one, we call it persisters. The need for persisters' concept is explained in the discussion at the end of this chapter.

Data for the case of glucose supplemented M9 media is very different from the case of maltose supplemented M9 media experiment. The phage population never had chance to outnumber the bacterial population, even similar low initial MOI was provided. The reason for

this difference in population dynamics is mostly due to the different burst size for the two different cases. Burst size is the number of phages produced by a single infected bacterium cell. Unfortunately, we never had chance to obtain accurate measurements for burst size of the cells grown and infected in the two different media. This parameter is the one we consider from simulation results. The populations' evolution profile is the most sensitive to the burst size. A small burst size will not allow phage population to outnumber the bacterial population and decimate it in the case of a low initial MOI population dynamics experiment. The two competing populations will grow at similar rates and reach steady state due to the carrying capacity of the system.

The simulation for the two experiments (figure 4-2) using our population dynamics model shows good agreement with the experimental data, considering the complexity of the two population interaction.

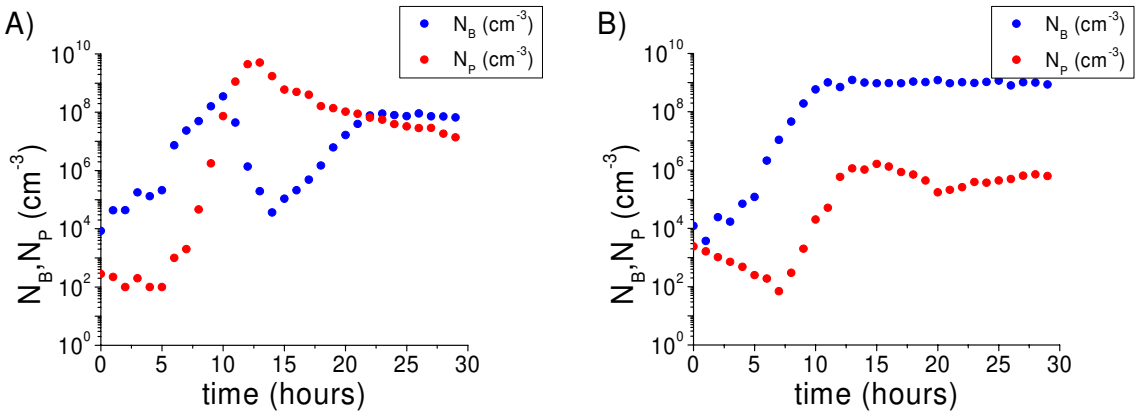

Figure 4-1 Experimental data for low initial MOI: A) maltose, B) glucose supplemented M9 media

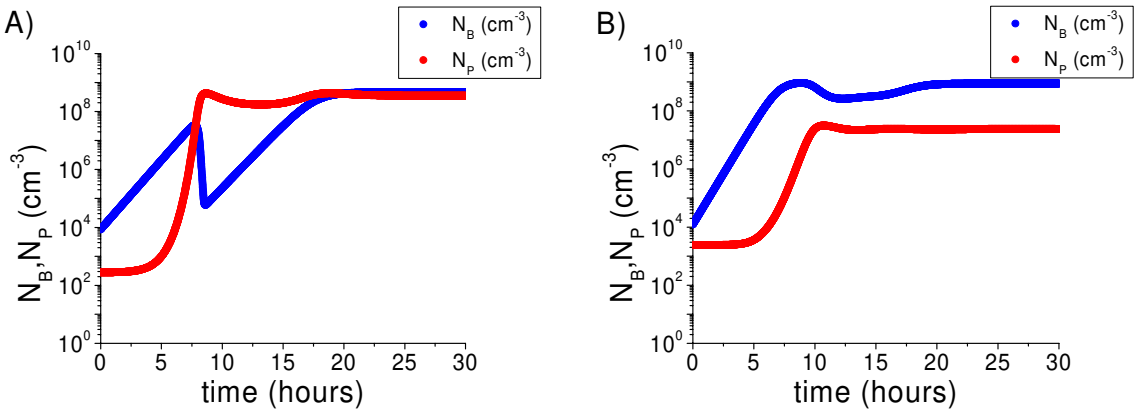

Figure 4-2 Simulation for low initial MOI: A) maltose, B) glucose supplemented M9 media

4.3.2 Parameters' values

The values of parameters used in simulating the two experiments are summarized in table 4-1. We assumed normal bacteria and persisters are growing at the same rate. To date we do not have experimental evidence proving otherwise. A direct measurement of persiters growth rate would be hindered by the switching rate of persisters into normal bacteria.

Table 4-1 Parameters' values

Parameters	Maltose supplemented M9	glucose supplemented M9
λ_N , λ_P	1.1 $hour^{-1}$	1.6 $hour^{-1}$
γ	$5 \cdot 10^{-8}$ cm^3/hour	$5 \cdot 10^{-8}$ cm^3/hour
α	10^{-4} $hour^{-1}$	10^{-4} $hour^{-1}$
β	.1 $hour^{-1}$	.2 $hour^{-1}$
m	30	3
ε	1.5 $hour^{-1}$	1.5 $hour^{-1}$

η	1 hour^{-1}	1 hour^{-1}

We performed high initial MOI experiments to generate killing curves, for which the normal bacteria population was decimated and the persisters' population prospered, under a constant phage pressure. The growth rate we observe in the recovery part of the killing curve is not the persisters' absolute growth rate λ_P, but an effective growth rate λ_{eff}, as seen in equation (4.7), which takes into account for the persisters turned into normal bacteria and killed due to constant phage pressure. The equation describing the persisters' population evolution, equation (4.2), can be written for the recovery part in a killing curve as following:

$$\frac{dN_{BP}}{dt} = \lambda_P N_{BP} - \beta N_{BP} + \alpha N_{BN} \ . \tag{4.6}$$

Notice the carrying capacity term is not needed here, since we are interested in the recovery part and not the saturation part. Also, $N_{BN}=0$ since the phage pressure is present. Therefore, equation (4.6) will become:

$$\frac{dN_{BP}}{dt} = \lambda_P N_{BP} - \beta N_{BP} = (\lambda_P - \beta) N_{BP} = \lambda_{eff} N_{BP} \ . \tag{4.7}$$

Unfortunately, the measurements of the effective growth rate for the two different media we performed population dynamics experiments in, are not accurate enough to resolve the difference between the absolute growth rate and the effective growth rate (data not shown). In other words, at this time we do not have the experimental means to obtain the switching rate of persisters into normal bacteria β. Therefore we have to rely on simulation for obtaining β.

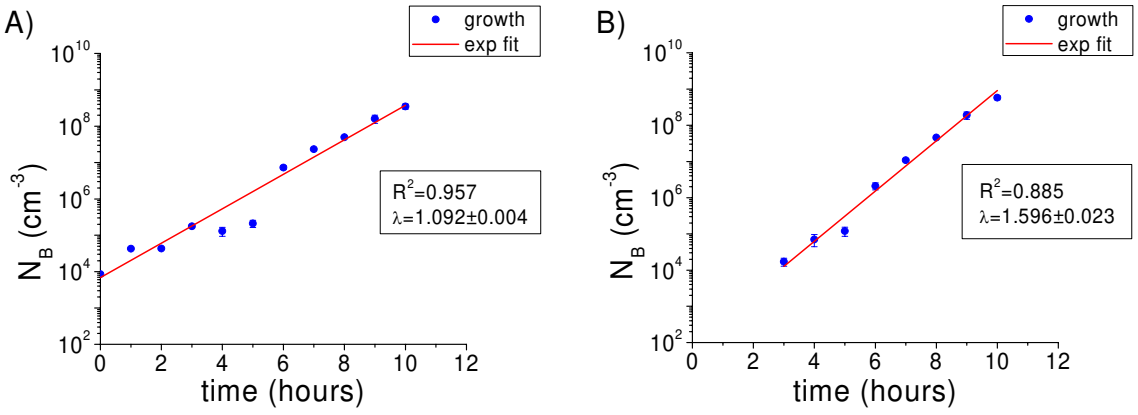

Figure 4-3 Bacterial growth rates for A) maltose, B) glucose supplemented M9 media

Measurement of the absolute growth of cells we used in population dynamics experiments, grown in the two media: maltose and glucose supplemented M9, are shown in figure 4-4. Notice that for both media the growth rate is higher than the effective growth rate encountered after killing and in the presence of phage pressure.

The switching rate α of normal bacteria into persisters is very low. We chose it of three orders of magnitude lower than β. The counterpart rate α for antibiotics persisters is also that small. The difference is in the growth rate λ_P of persisters to antibiotics, which is also small compared to the growth rate λ_N of normal bacteria (Balaban, Merrin et al. 2004).

The lysing rate is determined by the time bacteria need in order to produce phages after infection. The value can be obtained from one step growth experiments and corresponds to the latent period, which spans from the point of phage adsorption to the point at which host lysis occurs. The latent period is about 45 minutes for *E. coli* bacteria infected with lambda phages.

We introduce here η, the degradation rate of bacterial debris. This parameter describes how fast the bacterial debris looses their ability to inactivate lambda phages. This could be due to complete occupation of all receptors on the debris bacterial envelope. For our cell, we quantified

the number of receptors per cell, as it can be seen in chapter 3. Although this rate could be dependent on the instantaneous concentration of phages, we chose a fixed value which smooth out the simulation curves, following the experimental lines. A very off value for η will introduce oscillatory simulation curves, which could not be seen experimentally.

4.4 DISCUSSIONS

4.4.1 The need of persisters

High MOI experiments, in which the bacterial population is meant to be decimated, revealed a surprising feature. Even the bacterial population was outnumbered by phage population by a few orders of magnitude, not all bacteria got killed. There was always a small subpopulation able to survive the massive phage attack.

The survival statistics of a bacterium in the presence of phages can be calculated by using Poisson statistics. Let j_{cell} be the number of phages adsorbed by a bacterium per second, or in other words the number of phages that collide with a bacterium per second.

$$j_{cell} \equiv \frac{1}{N_B} \cdot \frac{dN_P}{dt} \ . \qquad (4.8)$$

On average, the number of phages absorbed is:

$$\frac{dN_P}{dt} = \gamma N_B N_P \ , \qquad (4.9)$$

where γ is the adsorption rate constant and N_B, N_P are the concentrations of bacteria, respectively phages. Therefore,

$$j_{cell} = \gamma N_p \ . \qquad (4.10)$$

Then, $j_{cell} \cdot dt$ is the elementary probability that the bacterium is hit by phages during time dt. If there are no collisions with phages, the bacterium will survive. If there are collisions with phages, they eventually terminate with infection of the bacteria. The probability that the bacterium is not hit in the first interval dt is $1-j_{cell} \cdot dt$. The question is: what is the chance for the bacterium to survive during time t? Or in other words, what is the probability that the bacterium is hit between t and t+dt (and not earlier)?

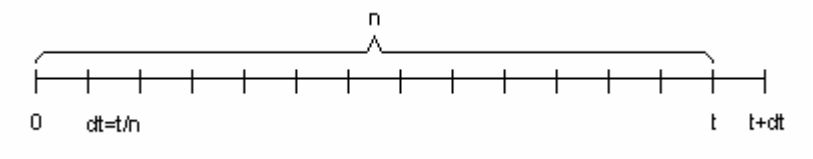

The probability that the bacterium is not hit in the first n intervals dt is: $(1-j_{cell} \cdot dt)^n$. The probability that the bacterium is not hit in the first n intervals dt, but is hit in the next one t+dt, is:

$$S(t;j_{cell}) \cdot dt = (1-j_{cell} \cdot dt)^n \cdot j_{cell} \cdot dt \ . \qquad (4.11)$$

Using $dt=t/n$ one can write:

$$S(t;j_{cell}) \cdot dt = \left(1-j_{cell} \cdot \frac{t}{n}\right)^n \cdot j_{cell} \cdot dt \ . \qquad (4.12)$$

Poisson process requires dt very small, therefore n very large, which leads to

$$S(t;j_{cell}) \cdot dt = e^{-j_{cell} \cdot t} \cdot j_{cell} \cdot dt \ . \qquad (4.13)$$

After integration, one can obtain the surviving probability for the bacterium during time t

$$S(t;j_{cell}) = e^{-j_{cell} \cdot t} \ . \qquad (4.14)$$

In our killing experiments, using equation (4.10) the value of j_{cell} is obtained as $\sim 10 s^{-1}$. The survival probability under such conditions over a period of time of 8 hours is practically zero:

$$S(8hours;10s^{-1}) = e^{-j_{cell}\cdot t} = e^{-10s^{-1}\cdot 8\cdot 3600s} = e^{-2.9\cdot 10^{5}} = 0 \ . \qquad (4.15)$$

However, experimentally we observed that even after 8 hours under such high phage pressure there is still a 10^3cells/ml surviving. This suggests that persistent bacteria to phage infection is a necessary concept in modeling the population dynamics for the bacteria-phage system. We believe the persistence against lambda phage infection is due to the lack of functional receptors, based on killing curve experiment performed with fluorescent lambda phages and the fluorescent images obtained in the experiment. In figure 4-5 one can see the phase and the fluorescent images A) and B) taken at 6 hours and C) and D) at 17 hours respectively, after killing with fluorescent lambda phages of cells grown in log phase (in glucose supplemented M9 media). Notice that after 6 hours from infection most of the bacteria are labeled and immobilized, meaning that they adsorbed fluorescent phages and got infected (see A) and B)), but after 17 hours from infection there are many unlabeled bacteria swimming around (see C) and D)) even though the phage pressure is still present. We believe these surviving bacteria to phage attack belong to the persisters' population, lacking functional receptors. Unfortunately, we cannot conclude if there are no receptors on the cell surface or if they are just nonfunctional.

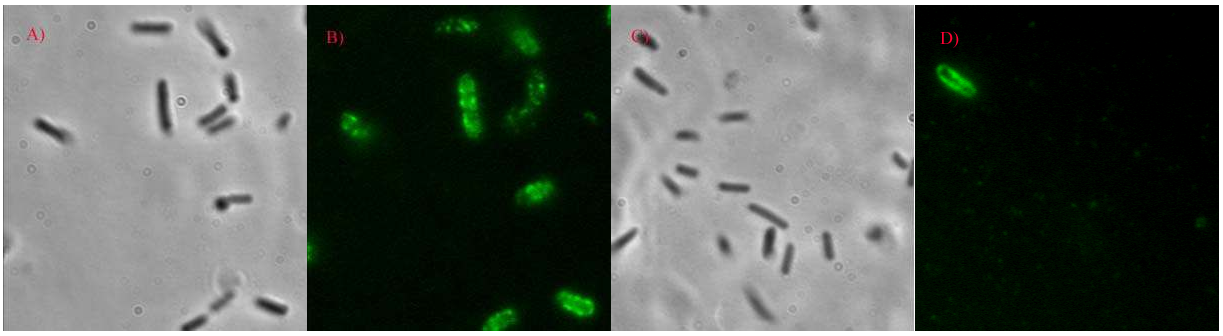

Figure 4-4 Persisters surviving phage killing: A), B) at 6 hours after killing most cells killed – labeled C), D) at 17 hours after killing the persisters population prospered and not infected – not labeled

By definition, persisters are the bacteria which survive the phage attack (or any other pressure), but they revert into normal cell at a certain rate. Beside persisters, there might be

mutants in the bacterial subpopulation that can survive the phage attack. Mutants don't revert back into normal cells. If they do the rate is negligible and not worth consideration here. There might be a third different category of bacteria in the surviving subpopulation, the category of lysogens. An infected bacterium that chooses the lysogenic cycle has immunity to superinfection to the same lambda phages. The lambda phage we use in our experiments comes from a lysogen which is heat inducible (*E. coli* C190, λcI857ind1 Sam7). Lambda phage λcI857 DNA expresses a repressor cI which is heat sensitive. At high temperature 36-42°C the repressor loses the ability to bind to the promoter and therefore the lytic cycles genes are expressed. We took advantage of this heat sensitive repressor and carried out the population dynamic experiments in 36°C, therefore the lysogenic state was very unlikely.

We even tested for lysogens in the bacterial population at the end of 5 different population dynamics experiments done in maltose supplemented M9 medium (as one sees in figure 4-1A) to make sure there are no lysogens involved. At the end of each experiment, after the interaction between bacteria and phage was stopped, 1 ml of incubation mixture was sample out. Cells were separated from phages by centrifugation and washed 5 times, then grown on LB plates. Among 50 colonies picked and grown in maltose supplemented M9 media overnight, none shown spontaneous phage release, but all shown lambda sensitivity when infected with new phages, which we believe that they are persisters turned back into normal bacteria on the plates. Therefore we rule out the lysogens, leaving only persisters and mutants as candidates for the population at the end of long population dynamics experiments. Another observation confirming that lysogens are not part of the surviving population is shown in figure 4-5. Lysogens have functional LamB receptors, therefore they should be labeled with fluorescent phages, but they are not.

We repeated the above experiment without getting rid of phages as we plated cells on LB. Therefore we had some phage pressure on the plate since the washing step was skipped and the mixture plated contained phages and cells in a ratio MOI=0.1. Then 20 colonies from this original plate were grown overnight in fresh maltose supplemented M9 media and checked for plaque formation after infection with lambda phages. 15 out 20 showed plaques, meaning they reverted to normal bacteria during the overnight growth. The other 5, which did not show sensitivity to phage infection were further studied for phage adsorption. Indeed, their adsorption curves show negligible phage adsorption compared to normal bacteria case, as one can see in figure 4-6. The phages diffuse to the cell membrane, but they cannot adsorb onto cell membrane, with the desorption rate being very high and the irreversible binding rate equal to zero according to our adsorption model. We believe these 5 colonies were mutants. We started to see them because of the phage pressure present on the plate. It is possible that a persister switching back into a normal cell gets killed due to the phage pressure on the plate, and therefore selecting for mutants. For a stronger phage pressure (i.e. very high MOI maintained by adding more phages), the selection for mutants was even stronger and most colonies shown no phage sensitivity. Therefore we can conclude that at end of population dynamic experiment, when the bacterial population coexists with phage population, there might be a fraction of mutants in addition to the persister population.

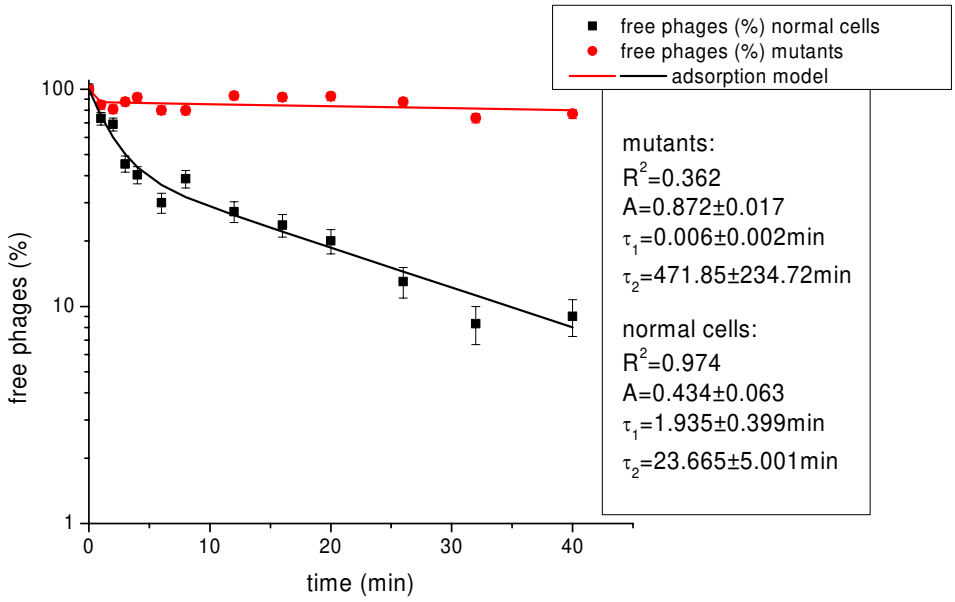

Figure 4-5 Phage adsorption onto normal cells vs. persisters

The strongest evidence proving the existence of persisters is the slow decrease in the bacterial population in the killing curve. The killing curve experiment is a population dynamics experiment with very high initial MOI, as one shown in figure 4-7. Most of the bacterial population is decimated very fast by the huge amount of phage pressure (MOI=50) as one can see in the figure below in region I. Then the killing becomes slower, as seen in the second part of the killing, region II. We believe this is due to the switching of persisters back into normal cells and get killed right away. Therefore the switching is limiting the killing.

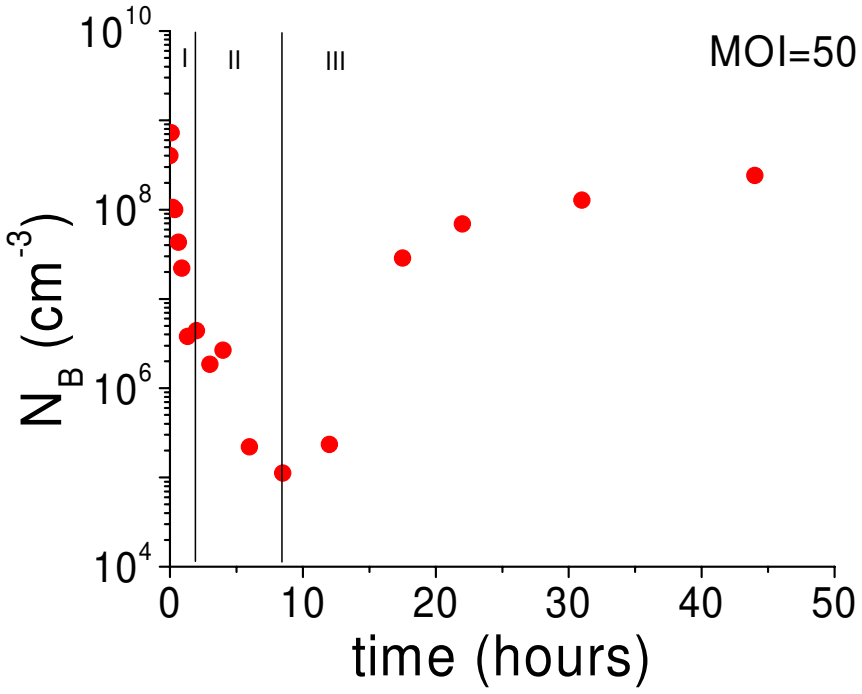

Figure 4-6 Killing curve at MOI=50 in glucose supplemented M9 media

4.4.2 Binary collision, the basic of our model

Using a binary collision concept to model interaction between bacteria and phages at low MOI seems intuitively correct, but using the same concept for the case of high MOI seems not obviously correct. In the case of our population dynamics experiments carried out in maltose supplemented M9 media, around time 12-13 hours MOI becomes huge as the phage population takes over. Let us estimate here the number of phages found in the volume of a single bacterium in the case of the highest phages concentration reached in our experiment. This concentration is $5 \cdot 10^{9} cm^{-3}$ and the volume of a single cell is approximately $3 \cdot 10^{-12} cm^{3}$ for a 4μm long bacterium. Therefore the probability to have a phage present in that small volume is .015. That means it is a very small chance of having two phages within a cell volume, which is the actual chance of

having two phages colliding with the same bacteria at the same instant. Therefore the binary collision concept is reasonable to explain the interaction between bacteria and phages in our population dynamics experiments.

4.4.3 Models with time delays

After adsorption of phages onto bacteria and the infection process is triggered, it takes the latent period until a phage crop is released. Therefore it would be more appropriate to use delay equation in describing the phage production. In our population dynamics model, we tried to mimic the delay by using the lysis rate ε. One can notice the shift of phage population peak to the right (later time) in our experimental data, which we believe is due to the delay in the production of phage. The same phage population peak is not shifted that much in the simulation, and therefore the killing part is stronger (faster) in the simulation than in the real experiment. Therefore we tried to improve our model by introducing delay equations.

Let us assume a phage infects a bacterium at time t-τ, and τ time later at t, the infected cell bursts and releases the new crop of phages. Therefore the phages produced at time t are due to the adsorption of phages onto bacteria at time t-τ. We do not need to keep track of complexes population, since we know this is just an intermediate population that ends up bursting and producing phages. Therefore we rewrote the population dynamics model replacing the phage production term $m\varepsilon N_{BN}^{*}$ with a delayed $m\gamma N_P N_{BN}$ term and also the debris term N_{BD} (sink for phages) replaced by a new meaning debris term N_{BD}^{*}. Indeed, the debris population here has a slightly different meaning than the one in the original model. Initially, the debris term was counting for dead bacteria with active receptors, still able to sink free phages. For the case of the

delay equations, the debris term is counted for all infected bacteria, dead or alive. In other words, as soon as a phage adsorbs (irreversibly) onto a bacterium, that bacterium becomes part of the debris and stays like that even after lysing. Therefore now the debris population has a broader meaning, it contains the original model populations for the complexes and for the debris. The reason for having originally these two populations separately described was because the complexes population was the phage production term. Since we got rid of one population, the complexes population N^*_{BN}, the delay equations version of our population dynamics model would include only four differential equations. The first two equations (4.1) and (4.2), describing the free normal bacteria population and the free persisters, are not changed at all, no need for delay. The phage population, equations (4.3) would be rewritten as the delay equation (4.18) in the delay equations model.

$$\frac{dN_{BN}(t)}{dt} = \left[\lambda_N \left(1 - \frac{N_{BN}(t) + N_{BP}(t)}{K} \right) - \gamma N_P(t) \right] N_{BN}(t) + \beta N_{BP}(t) - \alpha N_{BN}(t) \tag{4.16}$$

$$\frac{dN_{BP}(t)}{dt} = \lambda_P \left(1 - \frac{N_{BN}(t) + N_{BP}(t)}{K} \right) N_{BP}(t) - \beta N_{BP}(t) + \alpha N_{BN}(t) \tag{4.17}$$

$$\frac{dN_P(t)}{dt} = m\gamma \cdot N_{BN}(t-\tau) \cdot N_P(t-\tau) - \gamma \left(N_{BN}(t) + N^*_{BD}(t) \right) \cdot N_P(t) \tag{4.18}$$

$$\frac{dN^*_{BD}(t)}{dt} = \gamma \cdot N_{BN}(t) \cdot N_P(t) - \eta N^*_{BD}(t) \ . \tag{4.19}$$

This is the simplified version of the delay equation model considering the delay time τ fixed. More correctly, the delay time would be described by a distribution of values. In figure 4-8 we show the improvement in simulation of the population dynamics experiment performed in maltose supplemented M9 media with low initial MOI, by making use of delay equations.

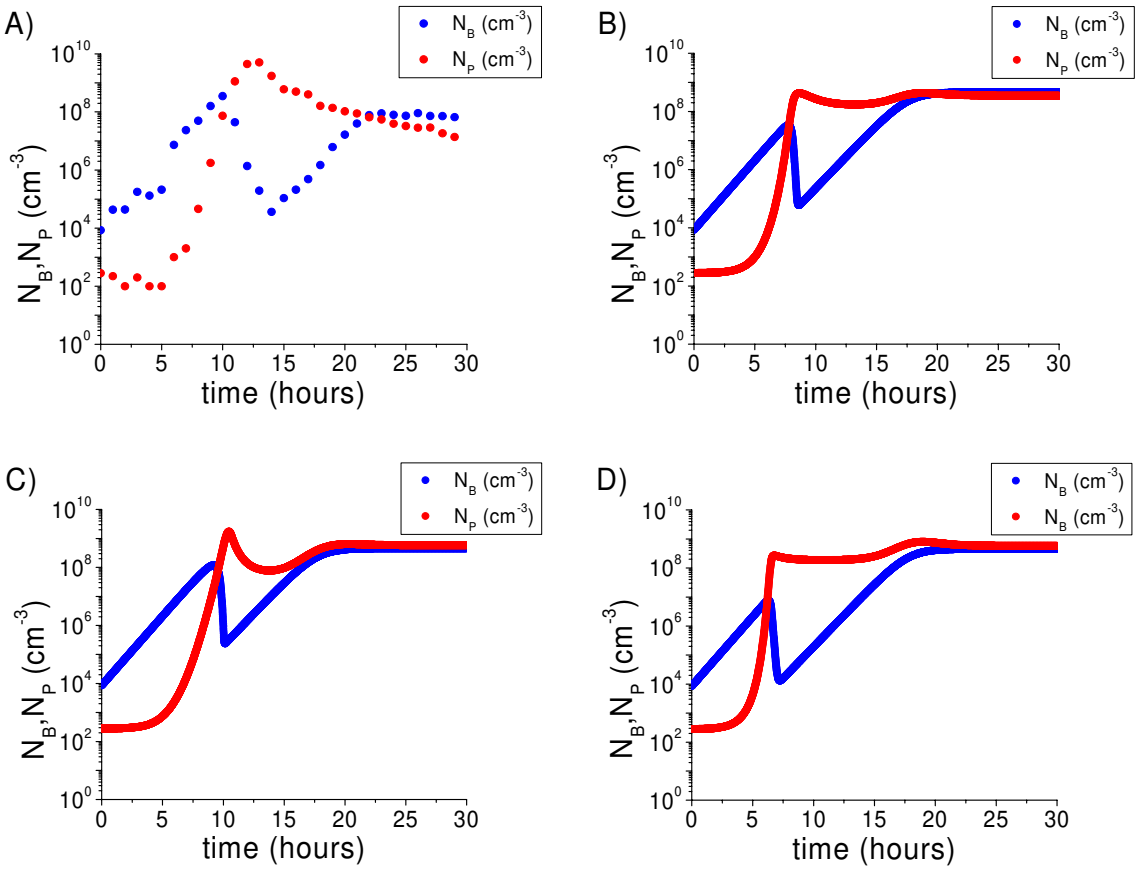

Figure 4-7 Population dynamics model A) experimental data B) original model C) delay equations model (delay 45 minutes) D) delay equations model (delay 0 minutes)

The delay equation model, as can be seen in figure 4-8 C), shows a better timing for the events during the population dynamics experiment. For example the phage population peak around time 12-13 hours in experimental data is matched better in the new simulation than the original one as seen in figure 4-8 B). As we already said, the original model is still mimicking delay in phage production via the bursting rate ε. For a delay equation model, with zero delay, and also no bursting rate to mimic delay, the timing would be faster, as can be seen in figure 4-8 D).

4.5 CONCLUSIONS

We were able to simulate the evolution of the population dynamics for the long-term interaction between lambda phage and its bacterial host in a co-habitual environment. A complex mathematical model, describing the dynamics of the two populations (bacteria and phages) was presented along with confirming experimental results. Surprising observations of persisting bacteria to phage infection were reported and discussed. The calculation of survival statistics of a bacterium in the presence of phages shows that the concept of persisting bacteria to phage infection is necessary to explain the phage-bacteria interaction at population level. There are three different kind of bacterial populations that can explain persistence to phage infection: persisters, lysogens and mutants. We ruled out the presence of lysogens in our experiments. We have strong evidences confirming the existence of persisters:

- killing curves show a second decay (slower) which imply that the persisters are switching back to normal bacteria and get killed by huge phage pressure (the switching back to normal is the limiting rate step)
- recovery of the phage sensitivity after regrowing the persister candidates

We also have fluorescence measurement confirming persistence to phage infection, due to lack of functional receptors.

APPENDIX

MATERIALS AND METHODS

.1 GROWING MEDIA AND BUFFERS

All media and buffers used in our work are standard (Ausubel, Brent et al. 1997).

M9 glucose/maltose (minimal growth media)

PartA 5X, per liter: 30g Na_2HPO_4, 15g KH_2PO_4, 5g NaCl, 15mg $CaCl_2$ (optional)

PartB 100X supplements, per 100ml (NOTE: filter by 0.45μm filter; do not autoclave!):

2.4g $MgSO_4 \cdot 7H_2O$ (0.1M), 20g carbon source (glucose/maltose), 10g Casamino Acids,

1ml of 0.5% vitamin B1

LB media (rich growing media), per liter: 10g peptone, 5g yeast extract, 2.5g NaCl, 1ml 1M NaOH

Lambda dilution buffer, per liter: 1.2g Tris (adjust pH to 7.4 using HCl), 0.6g NaCl, 4.9g $MgSO_4 \cdot 7H_2O$, .005% gelatin

Adsorption buffer: 10mM $MgSO_4$ (adjust pH to 7.4)

LB plates, per liter: 10g peptone, 15g agar, 5g yeast extract, 2.5g NaCl, 1ml 1M NaOH

Lambda plates, per liter: 10g peptone, 10g agar, 2.5g NaCl

Lambda top agar, per liter (NOTE: keep it liquid at 50°C degrees): 10g peptone, 7g agar, 2.5g NaCl

.2 BACTERIAL STRAINS

Thanks to the kindness of Dr. Roger Hendrix and Dr. Robert Duda from Biology Dept, University of Pittsburgh, we obtained Ymel strain, extensively used in our adsorption experiments. The common use of this strain in Dr. Hendrix Lab is as indicator bacteria for lambda phages.

Due to the kindness of Dr. Mary Berlyn, the curator of CGSC: *E. coli* Genetic Stock Center we obtained the bacterial strains: HfrG6 (CGSC#**:** 5388) and Hfr3000 (CGSC#**:** 259) Schwartz utilized in his adsorption measurements.

Due to the kindness of Dr. Jurgen Stolz, from Universität Regensburg, Germany, we obtained the propagation strain Q358 for the biotinylated lambda phages (Stolz, Ludwig et al. 1998).

We obtained λ lysogen from New England Biolabs, *E. coli* C190, λcI857ind1 Sam7, which is heat inducible lysogen that do not lyse unless uses chloroform.

.3 PHAGE STRAINS

We obtained lambda phages using *E. coli* C190, λcI857ind1 Sam7 from New England Biolabs, a heat inducible lysogen that needs chloroform for lysing, therefore high concentration of lambda phages can be reached (see the appendix).

We propagated biotinylated lambda phages (Stolz, Ludwig et al. 1998) by using the strain Q358 from Prof. Jurgen Stolz of Universitat Erlangen-Nurnberg, Germany. We used an amplification protocol for the biotinylated phages, so-called PDS (pick, dilute, streak) (see the appendix).

Due to the kindness of Dr. Hendrix Lab, Biology Dept, University of Pittsburgh, we obtained Ur-lambda phages (Hendrix and Duda 1992). This lambda related phage has extra jointed tail fibers that are absent from "wild" type lambda phage. Therefore compared to the "wild" type, Ur-lambda has expanded receptor specificity and adsorbs to *E. coli* cells faster. A technical issue should be mentioned here. For titering Ur-lambda phages by using soft agar overlay technique, the soft agar has to be freshly made and more dilute then the one use for the titering "wild" type lambda phages. Otherwise the plaques would be too small and difficult to count.

.4 EXPERIMENTAL PROCEDURES

Amplification of λ phages: PDS (pick, dilute and shake)

1. Make fresh plaques of phage (use fresh titer plate or streak plate from the phage stock plated in soft agar with appropriate host).

2. Preheat 1L of LB media in a 2.8L Fernbach Flask (put at 37˚C).

3. Using a Pasteur pipette, take three plugs from three separate plaques and add them to a test tube with 0.5 ml lambda dilution buffer.

4. Hold at 37˚C for 0.5-1 hour.

5. Add 0.5ml of stationary culture cells (cells are usually Ymel grown overnight in LB).

6. Incubate at 37˚C for 10-15 minutes.

7. Dilute mixture into 1 L of (preheated) LB media in a 2.8 L Fernbach Flask.

8. Incubate overnight (~15 hours) at 37˚C, with good aeration.

9. Lysis will possibly be evident (should, but maybe not).

10. Add at least 5ml of $CHCl_3$ and mix thoroughly for about 1 min, place on ice for at least 20 minutes, mix 2 to 3 times again. Tip flask and remove excess $CHCl_3$ using a 10ml pipette.

11. Treat lysate with DNase to reduce viscosity by adding Mg to 1mM (i.e., 1ml 1M MgSO4) and then adding DNase to about 0.1 μg/ml (i.e., 0.1ml of 1mg/ml DNase I). Raise the temperature to 30-37˚C for about 10 min.

12. Spin out debris at 7500rpm for 15 minutes.

13. Store cleared lysate at 4˚C until phage purification.

Purification of λ phages

1. First PEG precipitate the lysate containing λ phages by adding NaCl to 0.5M (~29.2g) and stirring to dissolve, then adding PEG 8000 to 10% (~100g) and stirring until dissolved. Let stand 30 min to over night then pellet by spinning at 8000rpm for 10-15 min. Pour off supernatant and drain pellets, then gently resuspend in small volume (2-3ml) of lambda dilution buffer (pellet undissolved material at low speed).

or

1'. Spin down the lysate in the ultra-centrifuge at 30,000g for 1h 30min and then gently resuspend in small volume (2-3ml) of lambda dilution buffer (pellet undissolved material at low speed).

2. Add CsCl to the concentrated phage volume (add 0.9g to 1ml to get a density of CsCl at 1.5g/ml). Use the refractometer to measure the desired CsCl density.

3. Load and seal the tubes (14ml)

4. Spin at 38,000g for 16 hours.

5. Extract the band by using needle syringe.

6. Dialyze three times, each time 10 hours against lambda dilution buffer.

Phage titering procedure

This method relies on plaques formation on indicator bacteria lawn by the agar overlay technique.

1. Grow overnight culture 5ml of the cells used for titering (indicator bacteria) in LB media.

2. Spin down the cells for 7 min at 3000rcf and resuspend in 2.5ml 10mM $MgSO_4$.

3. Perform a series dilution (usually one hundred fold dilution; or for more accuracy ten fold dilution) of a phage stock using the lambda dilution buffer to an appropriate concentration. The idea is to have 3-400 plaques on each lambda plate. In order to perform an one hundred fold dilution mix 10µl of lambda phage stock with 990µl lambda dilution buffer. In order to perform a ten fold dilution mix 100µl of lambda phage stock with 900µl lambda dilution buffer.

3. Incubate appropriate amount of phage (usually 0.1ml) with 0.1 ml cells at 37°C for 15 min.

4. Add 2.5 ml liquid lambda top agar kept at 50°C. Mix the infected cells with the agar and pour the mixture onto a lambda plate and spread it. NOTE: liquid lambda top agar hotter then 50°C can kill the infected bacteria, therefore no bacterial lawn, and no plaques.

5. Wait for the agar to solidify, invert the plates incubate at 37°C overnight.

6. Next day count the number of plaques and figure out the concentration of the phages. For example if the stock concentration C_0 has been seven times ten fold diluted: $C_7=C_0/10^7$, and the number of plaques of C_7 is 851 per 0.1 ml then C_7 = 8510/ml and $C_0 = 8.5x10^{10}$ /ml.

Adsorption experiment procedure

1. Grow **study bacteria** overnight in desired media. This is the strain of bacteria you want to study the adsorption for. Grow **indicator bacteria** overnight in LB (for phage titering), usually Ymel.

2. Re-grow **study bacteria** in log phase for 4 hours (for minimal media it takes longer).

3. Spin down **indicator bacteria** and **study bacteria** for 7min at 3000rcf

4. Resuspend **indicator bacteria** in 10^{-2}M $MgSO_4$ at roughly 10^9cells/ml

5. Resuspend **study bacteria** in 10^{-2}M $MgSO_4$. Using our optical density meter (the one we made in our lab) and the calibration file: **optical density M9 Maltose Glucose Ymel.xls** for

Ymel case adjust to the wanted bacterial concentration (roughly 100mV corresponds to 10^8cells/ml where 160mV is for total transmission light, see the note at the end). For other bacterial strains the optical density meter readings should not be very different. This is the **experimental bacterial stock**.

6. Titer the **experimental bacterial stock**.

7. Using a known concentration phage stock perform an appropriate series of dilution in lambda dilution buffer such that 10µl of 10^7phages/ml ends in 1.5ml lambda dilution buffer, that is 3-400 plaques on the final titering plates. This 1.5ml of diluted phage stock is the **experimental phage stock.**

8. Incubate 100µl of the **experimental phage stock** with 100µl of the **experimental bacterial stock** in 15ml glass tubes (add gently phages over bacteria using a cut tip to not introduce convection) for certain amounts of time in a well-controlled temperature water bath. It is known there is no feasible stirring at this scale (<1µm) (Purcell 1978). The adsorption is based on random diffusion, therefore cannot be increased by stirring.

9. Stop all reactions at once by a 54 fold dilution with 5.2ml 10^{-2}M $MgSO_4$ concentration solution in the same big glass tubes in which the incubation took place.

10. Sample roughly 1ml from each 15ml glass tube into a 1.5ml plastic centrifuge tube.

11. Spin all down for 1min at maximum speed ~16000 rcf, so the complexes cell-phage and all the other bacteria will pellet.

12. Sample out only 100µl from the top of the supernatant, which is free phages. Do not sample out from more then 4 centrifuge tubes at once. Spin again the others for 1min at maximum speed before sampling out from them to make sure the complexes did not resuspend.

13. Using standard titering (plaques formation on **indicator bacteria** lawn by the agar overlay technique) figure out the concentration of free phages for different incubation times.

NOTE: The **experimental bacterial stock** containing **study bacteria** has to be less concentrated then $5 \cdot 10^8$cells/ml, otherwise stopping the reactions is not efficient.

Population dynamics experiment procedure

1. Grow 5 ml of **study bacteria** overnight in desired media. This is the strain of bacteria you want to study the population dynamics for. Grow 20ml of **indicator bacteria** overnight in LB (for phage titering), usually Ymel.

2. Spin down **indicator bacteria** for 7min at 1000 rcf.

3. Resuspend **indicator bacteria** in 20ml of 10mM $MgSO_4$ at roughly 10^9cells/ml.

4. Put for incubation ~10^2 lambda phages/cc with ~10^4 cells/cc of **study bacteria** in 100cc in desired media and titer phages and bacteria.

5. Every hour sample out 1cc of the incubation mixture and separate the cells from the phages by centrifugation at 7000 rcf for 5 minutes. Do your best for separating the supernatant from the pellet (be sure the pellet is not disturbed and get rid of as much as possible supernatant).

6. Perform an appropriate series of dilutions using lambda dilution buffer and titer phages (supernatant).

7. Resuspend the pellet and perform an appropriate series of dilutions using 10mM MgSO4 and titer cells.

Biotinylation activity detection

For this task we used a New England BioLabs product Phototope® -Star Detection Kit (catalog #N7020S). Phototope® Chemiluminescent Kits are designed for the non-radioactive detection of nucleic acids and proteins. These kits offer the opportunity to replace radioactivity method with a fast, sensitive and safe alternative. Phototope detection with CDP-Star is based on chemiluminescence, an enzymecatalyzed reaction that emits a blue light. In the Phototope Detection Kits for proteins, biotin associated with the target protein provides the handle for the chemiluminescent detection. Biotinylated protein is detected on a membrane support by first exposing the membrane to streptavidin, which binds to the biotinylated protein. Next, biotinylated alkaline phosphatase is added, which binds to the streptavidin, resulting in the creation of a conjugate between the alkaline phosphatase and the protein on the membrane. In the final step, the CDP-Star™ reagent is added. Alkaline phosphatase catalyzes the removal of the phosphate from the CDP-Star (phenylphosphate substituted 1,2 dioxetane) to yield a moderately stable intermediate which then spontaneously decays, emitting light at 461 nm. The emitted light is detected by exposing the membrane to x-ray film for 1 to 10 minutes. The protocol presented here will allow detection of biotinylated protein on western blots.

Kit Components

Streptavidin: 1.0mg at a concentration of 1.0mg/ml (1000X).

Biotinylated Alkaline Phosphatase: 0.5mg at a concentration of 0.5mg/ml (1000X).

CDP-Star: 1.0ml of a 25mM solution.

CDP-Star Assay Buffer: 20ml of 2-amino-2-methyl-1-propanol buffer supplied as a 25X liquid concentrate.

Solutions:

Blocking Solution: 5% SDS, 125mM NaCl, 25mM sodium phosphate, pH 7.2

Wash Solution I: 0.5% SDS, 12.5mM NaCl, 2.5mM sodium phosphate, pH 7.2

Wash Solution II: 10mM Tris-HCl, 10mM NaCl, 1mM MgCl2, pH 9.5

Phototope Detection Protocol:

1. Blocking step

Add to the hybridization bag 0.1 ml of Blocking Solution per cm^2 membrane. Incubate for 5 minutes at room temperature with moderate shaking. Drain the solution before the next step.

2. Streptavidin incubation

Determine the necessary volume of diluted solution based on using 0.05ml of diluted streptavidin per cm^2 of membrane. Prepare this volume by diluting the stock solution with Blocking Solution to a final concentration of 1 μg streptavidin/ml (1:1000 dilution). Incubate for 5 minutes at room temperature with moderate shaking. Drain the solution before next step.

Dilute 5μl of streptavidin stock solution to 5ml with blocking solution.

3. Wash 2 times using Wash Solution I

Use 0.5 ml Wash Solution I per cm^2 of membrane. Wash twice, 5 minutes each, at room temperature with moderate shaking. Drain and discard the solution after each wash.

4. Biotinylated Alkaline Phosphatase incubation

Determine the necessary volume of diluted phosphatase based on using 0.05ml of diluted phosphatase per cm^2 of membrane. Prepare this volume by diluting the stock solution 1:1000 with Blocking Solution to a final concentration of 0.5μg/ml.

Incubate for 5 minutes at room temperature with moderate shaking. Drain the solution before next step.

5. Wash 1 time using Blocking Solution

Use 0.5ml Blocking Solution per cm^2 of membrane. Wash once for 5 minutes, at room temperature with moderate shaking. Drain and discard the solution.

6. Wash 2 times using Wash Solution II

Use 0.5ml of 1X Wash Solution II per cm^2 of membrane. Wash twice, 5 minutes each, at room temperature with moderate shaking. Drain and discard the solution after each wash.

7. Detecting the biotinylated protein

The CDP-Star reagent is supplied as a 25mM stock solution and should only be diluted immediately before use. CDP-Star Diluent is supplied as a 25X stock solution. Dilute CDP-Star stock solution 1:200.

a. Dilute the 25X CDP-Star Assay Buffer with Milli-Q™ water to a 1X concentration.

b. Determine the amount of diluted CDP-Star needed and prepare this quantity immediately before use. Use 0.025ml of diluted CDP-Star reagent per cm^2 membrane. The diluted CDP-Star reagent is prepared by diluting the 25mM CDP-Star stock solution with the 1X CDP-Star Diluent.

Dilute 25µl of 25mM CDP-Star stock solution to 2.5ml with 1X CDP-Star Diluent.

c. Add the diluted CDP-Star reagent to the hybridization bag. Incubate for 5 minutes at room temperature with moderate shaking. Open bag and drain as thoroughly as possible.

d. After draining the majority of the reagent off the membrane, smooth out any wrinkles and reseal the bag. Remove any liquid from the outside of the bag and expose to x-ray film. It is important to achieve close, uniform contact between the film and the membrane to obtain sharp images.

BIBLIOGRAPHY

Adam, G. and M. Delbruck (1968). Structural Chemistry in Molecular Biology; chapter: Reduction of dimensionality in biological diffusion processes, W.H.Freeman and Co.

Ausubel, F. M., R. Brent, et al. (1997). Short protocols in molecular biology, John Wiley & Sons.

Axelrod, D. and M. D. Wang (1994). "Reduction-of-Dimensionality Kinetics at Reaction-Limited Cell Surface Receptors." Biophys. J. **66**(3): 588-600.

Balaban, N. Q., J. Merrin, et al. (2004). "Bacterial Persistence as a Phenotypic Switch." Science **305**: 1622-1625.

Berg, H. and E. Purcell (1977). "Physics of Chemoreception." Biophy. J. **20**: 193-219.

Berg, H. C. (1993). Random walk in biology, Princeton Univ Press.

Beveridge, T. J. (1999). "Structures of Gram-Negative Cell Walls and Their Derived Membrane Vesicles." J. Bacteriol. **181**: 4725-4733.

Charbit, A. and M. Hofnung (1985). "Isolation of different bacteriophages using the LamB protein for adsorption on Escherichia coli K-12." J. Virol. **53**: 667-671.

Choi-rhee, E., H. Schulman, et al. (2004). "Promiscuous protein biotinylation by Escherichia coli biotin protein ligase." Protein Science **13**: 3043-3050.

Clement, J. M. and M. Hofnung (1981). "Gene sequence of the lambda receptor, an outer membrane protein of E.coli K12." Cell **27**: 507-514.

Crick, F. and J. Watson (1970). "Central Dogma of Molecular Biology." Nature **227**: 561-563.

d'Herelle, F. (1917). "Sur un microbe invisible antagonists des Bacilles Dysenteriques." Compt. rend. **165**: 373-375.

Delbruck, M. (1940). "Adsorption of bacteriophages under various physiological conditions of the host." J. Gen. Physiol. **23**: 631-642.

Elliott, J. and W. Arber (1978). "E. coli K-12 pel mutants, which block phage lambda DNA injection, coincide with ptsM, which determines a component of a sugar transport system." Mol Gen Genet. **161**(1): 1-8.

Evilevitch, A., L. Lavelle, et al. (2003). "Osmotic pressure inhibition of DNA ejection from phage." Proc. Natl. Acad. Sci. U.S.A. **100**: 9292-9295.

Feilmeier, B. J., G. Iseminger, et al. (2000). "Green fluorescent protein functions as a reporter for protein localization in E.coli." J. Bacteriol. **182**: 4068-4076.

Ferenci, T. and W. Boos (1980). "The role of the E.coli receptor in the transport of maltose and maltodextrins." J. Supramol. Struct. **13**: 101-116.

Fischer, H., I. Polikarpov, et al. (2004). "Average protein density is a molecular-weight-dependent function." Protein Sci. **13**: 2825-2828.

Fuerst, C. R. and H. Bingham (1978). "Genetic and physiological characterization of the J gene of bacteriophage lambda." Virology **87**: 437-458.

Furusawa, C., T. Suzuki, et al. (2005). "Ubiquity of Log-normal Distributions in Intra-cellular Reaction Dynamics." Quantitative biology online **1**.

Gibbs, K., D. Isaac, et al. (2004). "Complex spatial distribution and dynamics of an abundant Escherichia coli outer membrane protein, LamB." Molecular Microbiology **53**: 1771-1783.

Glasstone, S., K. J. Laidler, et al. (1941). The theory of rate processes. New York, McGraw-Hill Book Co. Inc.

Harrison, D. P. and V. C. Bode (1975). "Putrescine and certain polyamines can inhibit DNA injection from bacteriophage lambda." J. Mol. Biol. **96**: 461-470.

Hendrix, R. W. and R. L. Duda (1992). "Bacteriophage lambda PaPa: not the mother of all lambda phages." Science **258**: 1145-1148.

Hershey, A. D. and M. Chase (1952). " Independent functions of viral protein and nucleic acid in growth of bacteriophage." J. Gen. Physiol. **36**: 39-56.

Ishii, J. N., Y. Okajima, et al. (1981). "Characterization of lamB protein from the outer membrane of Escherichia coli that forms diffusion pores selective for maltose-maltodextrins." FEBS Lett. **134**: 217-220.

Katsura, I. (1983). Lambda II; chapter: Tail Assembly and Injection. Cold Spring Harbor Laboratory, NY, Hendrix, Roberts, Stahl, Weisberg.

Kussell, E., R. Kishony, et al. (2005). "Bacterial Persistence: A Model of Survival in Changing Environments." Genetics **169**: 1807-1814.

Mackay, D. J. and V. C. Bode (1976). "Events in lambda injection between phage adsorption and DNA entry." Virology **72**: 154-166.

McCloskey, M. A. and M. Poo (1986). "Rates of Membrane-associated Reactions: Reduction of Dimensionality Revisited." J. Cell Biol. **102**(1): 88-96.

Montag, D., H. Schwartz, et al. (1989). "A Component of the Side Tail Fiber of Escherichia coli Bacteriophage A Can Functionally Replace the Receptor-Recognizing Part of a Long Tail Fiber Protein of the Unrelated Bacteriophage T4." J. Bacteriol. **171**(8): 4378-4384.

Mousset, S. and R. Thomas (1969). "Ter, a Function which generates the Ends of the Mature Chromosome." Nature **221**: 242-244.

Murialdo, H. (1991). "Bacteriophage Lambda DNA Maturation and Packaging." Annu. Rev. B.iochem. **60**: 125-153.

Nakae, T. and J. N. Ishii (1982). "Molecular weight and subunit structure of LamB proteins." Ann. Inst. Pasteur Microbiol. **133A**: 21-25.

Neuhaus, J. (1982). "The receptor protein of phage lambda: purification, characterization and preliminary electrical studies in planar lipid bilayers." Ann Microbiol (Paris) **133A**: 27-32.

Ptashne, M. (1986). A Genetic Switch: Gene Control and Phage, Cell Press; Blackwell Scientific Publications.

Purcell, E. M. (1978). "The Effect of Fluid Motions on the Absorption of Molecules by Suspended Particles." J. Fluid. Mech. **84**: 551-559.

Roa, M. (1979). "Interaction of bacteriophage K10 with its receptor, the lamB protein of Escherichia coli." J. Bacteriol. **140**: 680-686.

Royama, T. (1992). Analytical Population Dynamics. New York, Chapman & Hall.

Sanger, F., A. R. Coulson, et al. (1982). "Nucleotide sequence of bacteriophage lambda DNA." J. Mol. Biol. **162**(729-773).

Scandella, D. and A. Werner (1974). "An Escherichia coli mutant which inhibits the injection of phage λ DNA." Virology **58**(2): 504-513.

Schirmer, T., T. A. Keller, et al. (1995). "Structural basis for sugar translocation through maltoporin channels at 3.1 Å resolution." Science **267**: 512-514.

Schwartz, M. (1975). "Reversible interaction between coliphage lambda and its receptor protein." J. Mol. Biol. **99**: 185-201.

Schwartz, M. (1976). "The Adsorption of Coliphage Lambda to its Host: Effect of Variations in the Surface Density of Receptor and in Phage-Receptor Affinity." J. Mol. Biol. **103**: 521-536.

Schwartz, M. (1980). Virus receptors; chapter: Interaction of Phages with their Receptor Proteins, Chapman and Hall - 1980.

Schlesinger, M. (1960). "Adsorption of bacteriophages to homologous bacteria" Papers on Bacterial Viruses, Little Brown and Co.

Stent, G. S. (1963). Molecular Biology of Bacterial Viruses, H. Freeman and Co.

Stolz, J., A. Ludwig, et al. (1998). "Bacteriophage lambda surface display of a bacterial biotin acceptor domain reveals the minimal peptide size required for biotinylation." FEBS Lett. **440**: 213-217.

Thirion, J. P. and M. Hofnung (1972). "On some genetic aspects of phage lambda resistance in Escherichia coli K12." Genetics **71**: 207-216.

Twort, F. (1915). "An investigation on the nature of ultramicroscopic viruses." Lancet **2**: 1241-1243.

von Smoluchowski, M. (1917). "Versuch einer mathematischen Theorie der Koagulationskinetik kolloider Lösungen." Z. Phys. Chemie. **92**: 129-168.

Wang, J., M. Hofnung, et al. (2000). "The C-terminal portion of the tail fiber protein of bacteriophage lambda is responsible for binding to LamB, its receptor at the surface of Escherichia coli K-12." J. Bacteriol. **182**: 508-512.

Weigle, J. (1966). "Assembly of phage lambda in vitro." Proc. Natl. Acad. Sci. U.S.A. **55**: 1462-1466.

Weigle, J. (1968). "Studies on head-tail union in bacteriophage lambda." J. Mol. Biol. **33**: 483-489.

Werts, C., V. Michel, et al. (1994). "Adsorption of Bacteriophage Lambda on the LamB Protein of Escherichia coli K-12: Point Mutations in Gene J of Lambda Responsible for Extended Host Range." J. Bacteriol. **176**(4): 941-947.

Williams, N., D. K. Fox, et al. (1986). "Pel, the protein that permits lambda DNA penetration of Escherichia coli, is encoded by a gene in ptsM and is required for mannose utilization by the phosphotransferase system." Proc Natl Acad Sci **83**(23): 8934-8938.

Wu, X. L. and A. Libchaber (2000). "Particle diffusion in a quasi-two-dimensional bacterial bath." Phys. Rev. Lett. **84**: 3017-3020.